

DEVELOPMENT OF MICROFLUIDIC DEVICES FOR BIOPHARMACEUTICAL
PRODUCTION AND BIOTOXIN DETECTION

A Dissertation

Presented to the Faculty of the Graduate School

of Cornell University

In Partial Fulfillment of the Requirements for the Degree of

Doctor of Philosophy

by

Sowmya Kondapalli

May 2011

© 2011 Sowmya Kondapalli

ALL RIGHTS RESERVED

DEVELOPMENT OF MICROFLUIDIC DEVICES FOR BIOPHARMACEUTICAL PRODUCTION AND BIOTOXIN DETECTION

Sowmya Kondapalli, Ph. D.

Cornell University 2011

In this work, we present two different applications of microfluidic control. In the first application, we have developed a microfluidic device that has the potential to automate combinatorial protocols like protein refolding, impacting the biopharmaceutical industry. This device uses microfluidic valves and pumps that can be operated in an automated fashion for fluidic control. We performed refolding experiments on the protein β -galactosidase and showed on-chip quantification of refolding yield using a fluorometric assay. In the second application, we have developed a microfluidic immunobiosensor with an integrated preconcentration system to improve the detection sensitivity. A nanoporous membrane fabricated in-situ using photopolymerization technique inside glass microchannels acts as the preconcentration system. Analytes were electrophoretically concentrated at the membrane and the concentrated bolus was eluted towards a detection region downstream. We performed proof-of-principle experiments using biotin-streptavidin binding to show the improvement in detection sensitivity of this device as opposed to a device that does not include a preconcentration system. Using this device, we also showed a detection limit of 1.6×10^5 PFU/ml for Feline Calicivirus (FCV), which is a model system for human enteric virus. This device has potential to serve as an early detection system for such enteric viruses in environmental water samples.

BIOGRAPHICAL SKETCH

Sowmya was born in 1984 in Hyderabad, India. Although both her parents have Ph.D.s in plant sciences, she took a keen interest in mathematics since childhood and was greatly inspired by her grandfather who was a gold medalist in mathematics.

Sowmya began her undergraduate studies in Mechanical Engineering in 2001 at the Indian Institute of Technology (IIT) Madras, Chennai, India. She chose Biomedical Engineering as her minor field of study. It was during a bioengineering talk on the use of stents and catheters in heart surgeries that she was greatly inspired to work at the interface of engineering and biology. She graduated in 2005 from IIT Madras and was awarded the merit prize for the best senior year project in Mechanical Engineering. She joined Prof. Kirby's group at Cornell University in fall 2005.

Apart from academics, Sowmya has participated in various volunteer and outreach activities. She also takes interest in watching cricket, listening to Indian music and cooking.

After completing her degree, Sowmya plans to join the industry to get some exposure before she starts her teaching career.

ACKNOWLEDGEMENTS

First and foremost, I would like to express my gratitude to my parents, Dr. Nagamani and Dr. Satya Mohan Kondapalli, who have been a constant source of support and encouragement throughout my life.

I would like to thank my advisor and committee chair, Prof. Brian Kirby, for his guidance and insight throughout this process. His depth of knowledge has always been a source of inspiration and his emphasis on efficient communication has helped me in improving my presentation and technical writing skills. He has been an excellent mentor and I am very grateful for this learning experience. I would also like to thank my committee members, Prof. Antje Baeumner and Prof. Lance Collins, for their help and perspective they have lent to this work.

I am grateful to John Connelly for all the useful discussions and countless hours of assistance on the virus detection project. I would also like to express my gratitude to Prof. David Putnam for help with the protein refolding project and Prof. John Parker for providing virus and antibody stock.

My colleagues in Kirby lab have helped create a friendly and enjoyable learning atmosphere. I would particularly like to acknowledge Ben Hawkins, Vishal Tandon and Alex Barbati for their help and advice. I would also like to thank Mike Arszman, Dino Castellucci and Prashant Sundar for their lab assistance on the protein refolding work.

Finally, I would like to thank Marcia Sawyer for her help throughout my stay here at Cornell. I would also like to thank my friends and housemates who have made this place my home away from home, my big extended family in India and most specially my husband Kartik Yellepeddi, for believing in me.

TABLE OF CONTENTS

Biographical Sketch	iii
Acknowledgements	iv
Table of Contents	v
List of Tables	viii
List of Figures	ix
1 INTRODUCTION.....	1
1.1 Refolding of β -galactosidase in a microfluidic device	1
1.1.1 Production of recombinant proteins in the biopharmaceutical industry.	1
1.1.2 Protein refolding.	2
1.1.3 Microfluidic devices for protein refolding.	4
1.2 Development of antibody-based microfluidic biosensors for environmental water sampling.	6
1.2.1 Enteric viruses in environmental water samples.	6
1.2.2 Detection of enteric viruses	6
1.3 Taylor-Aris dispersion	11
Bibliography.....	15
2 REFOLDING OF β-GALACTOSIDASE: MICROFLUIDIC DEVICE FOR REAGENT METERING AND MIXING AND QUANTIFICATION OF REFOLDING YIELD.....	22
2.1 Abstract	22
2.2 Introduction	22
2.3 β -Galactosidase refolding	24
2.4 Materials and methods	25
2.4.1 Reagents	25
2.4.2 Device fabrication	25
2.4.3 Device preparation	27
2.4.4 Denaturing and refolding protocols	27
2.4.5 Activity assay.	27
2.4.6 Fluorescence measurements	28
2.4.7 Image processing	28
2.5 Device design.	29
2.6 Results.	31
2.6.1 Determination of optimum pumping frequency	31
2.6.2 Reagent mixing in the annulus	31
2.6.3 Determination of optimum FDG incubation time	33
2.6.4 Determination of optimum dilution ratio	34
2.6.5 Calibration of fluorescence intensity in a PDMS microchannel	35

2.6.6	Quantifying active protein content in denatured and refolded samples on-chip	35
2.7	Discussion	36
2.8	Conclusion.	38
2.9	Acknowledgements.	38
Bibliography.		39
3	INTEGRATED MICROFLUIDIC PRECONCENTRATOR AND IMMUNOBIOSENSOR	43
3.1	Abstract	43
3.2	Introduction	43
3.3	Experimental methods	46
3.3.1	Fabrication of microfluidic channels	46
3.3.2	Wafer bonding	47
3.3.3	Membrane fabrication and surface treatment	48
3.3.4	Liposome and magnetic bead preparation	49
3.3.5	Sample loading, concentration and detection	50
3.4	Results	52
3.4.1	Electrophoretic concentration of fluorescent liposomes.	52
3.4.2	Integrated concentration and detection experiments	54
3.4.3	Comparison of device performance with and without concentration	55
3.5	Discussion	56
3.6	Conclusion	58
3.7	Acknowledgements.	59
Bibliography		60
4	MICRO-TOTAL ANALYSIS SYSTEM FOR VIRUS DETECTION: MICROFLUIDIC PRECONCENTRATION COUPLED TO LIPOSOME-BASED DETECTION.	65
4.1	Abstract	65
4.2	Introduction	66
4.3	Materials and methods	69
4.3.1	Biotinylation of antibodies	69
4.3.2	Preparation of capture beads	69
4.3.3	Preparation of streptavidin-conjugated liposomes	69
4.3.4	Microtiter plate liposome immunoassay for antibody selection.	70
4.3.5	Concentration and detection of FCV	71
4.3.6	Detection of FCV without electrokinetic concentration	73
4.4	Results and discussion	75
4.4.1	Selection of antibodies and assay optimization	75
4.4.2	Comparison of FCV detection with and without electrokinetic concentration.	77

4.5	Conclusion	79
4.6	Acknowledgements	80
Bibliography.....		81
5	CONCLUSION	85
5.1	Summary of accomplishments	85
5.2	Future work	88
Bibliography.....		92

LIST OF TABLES

1.1	Comparison of different techniques for virus detection.....	9
-----	---	---

LIST OF FIGURES

1.1	Induced Poiseuille flow in microchannels due to electrokinetic pump action.....	13
2.1	Schematic of channel layout, pump and valve action.....	30
2.2	Picture of microfluidic device integrated to manifold.....	30
2.3	Volume injection rate vs. actuation frequency.....	32
2.4	Snapshots of device during mixing.....	32
2.5	Fluorescence signal vs. FDG – β -Galactosidase incubation time.....	33
2.6	Fluorescence intensity vs. dilution in renaturing buffer.....	34
2.7	Calibration curve of β -Galactosidase concentration vs. intensity.....	35
2.8	Comparison of denatured and refolded samples on-chip.....	36
3.1	Image of the integrated glass microfluidic device.....	46
3.2	Schematic of device for biotin-streptavidin binding experiments.....	51
3.3	Image sequence showing liposome concentration and elution.....	53
3.4	Concentration factors during liposome concentration vs. time.....	53
3.5	Image of fluorescent liposomes captured at the bead bed.....	55
3.6	Snapshots of region of interest during OG injection.....	55
3.7	Fluorescence intensity profiles during OG injection.....	57
3.8	Comparison of effect of preconcentration on device performance.....	57
4.1	Image of the integrated microfluidic device for virus detection.....	72
4.2	Schematic of analyte binding and liposome lysis.....	72
4.3	PDMS device without preconcentration module.....	74
4.4	Dose-response curve for different monoclonal probe antibodies.....	75
4.5	Optimized assay for FCV detection in cell culture lysate.....	76
4.6	Dose-response curve for FCV detection with preconcentration.....	77
4.7	Dose-response curve for FCV detection without preconcentration....	78

CHAPTER 1

INTRODUCTION

In this work, we present two different applications of microfluidic control. In the first application, fluidic injection and mixing is controlled by valves and pumps and this device is used for automating combinatorial protocols like protein refolding. The rotary mixer used in this device helps to overcome the long mixing times characteristic of microfluidic flows which are low Reynolds number and high Peclet number flows. In the second application, fluidic control is achieved using electric fields in conjunction with a nanoporous membrane to concentrate analytes and this is combined with a downstream detection system. The application of this device is to detect the presence of viruses in water samples. The electrophoretic preconcentration used in this device helps to improve the limit of detection of the integrated biosensor.

1.1 Refolding of β -galactosidase in a microfluidic device

1.1.1 Production of recombinant proteins in the biopharmaceutical industry

In the biopharmaceutical industry, bacterial genome is manipulated using recombinant DNA technology to produce pharmacologically useful peptides like the human insulin polypeptides [1]. Bacterial systems like *E. coli* are commonly used as hosts for the production of such recombinant proteins [2]. To overexpress the production of recombinant proteins, these bacteria are induced using reagents like isopropyl β -D-thiogalactopyranoside, which is an inducer of the lac promoter [3]. This over-

expression leads to the formation of misfolded protein aggregates called inclusion bodies [4]. Aggregation of proteins into inclusion bodies maybe due to the limiting amounts of molecular chaperones (needed to properly refold proteins to their native state) in such over-expressed systems [5]. When non-physiological amounts of proteins are produced, the aggregation of the folding intermediates occurs due to interaction of the exposed hydrophobic surfaces before protein folding is completed. The formation of inclusion bodies is a bottleneck in protein production as the refolding protocols to convert the non-functional inclusion bodies to their functional native state are complex. The solution conditions, like buffers and the right pH conditions, to properly refold proteins are not known *a priori* and choosing these solution conditions is a highly empirical process.

1.1.2 Protein refolding

The process of refolding refers to the conversion of the misfolded protein aggregates or inclusion bodies into the folded native state. The native and functional three-dimensional structure of a protein under a given set of conditions (solvent, pH, ionic strength, temperature etc.) is determined by its amino acid sequence (or the primary structure) [6]. This native state also corresponds to the one for which the Gibbs free energy of the system is the lowest [6]. In the folded state, proteins have their nonpolar side chains buried in the interior, which constitutes the hydrophobic core, while the polar groups occupy the solvent-exposed surface, constituting the hydrophilic exterior. The formation of intramolecular hydrogen bonds and disulphide linkages further enhances the stability of the protein. These various interactions like hydrophobic effects, hydrogen bonds and disulphide linkages drive the folding mechanism of the protein, collapsing it to its native state [7].

The main challenge in refolding proteins is the competing kinetics between aggregation and refolding [8]. Aggregation is a strong function of the initial protein concentration. As a result, refolding is performed in a renaturing medium at very high dilutions. The first step in the refolding protocol involves solubilizing the inclusion bodies into individual protein strands using strong denaturants like 6M guanidinium chloride or 6-8M urea. These reagents are strong chaotrophs, which shield the charged groups of the proteins and disrupt the stabilizing intramolecular interactions like hydrogen bonds and hydrophobic effects, thereby solubilizing the aggregated proteins. The solubilized proteins are then diluted in a renaturing medium which contains various artificial chaperones which are chemicals which help to properly refold the individual protein strands into their native state, while keeping them solubilized. Examples of these artificial chaperones include non-denaturing concentrations of chaotrophs (which prevent hydrophobic interactions between folding intermediates), zwitterionic detergents and different salts. Selecting the right combination of these chaperones is a combinatorial process [9].

We performed refolding experiments on the protein β -galactosidase, which is an essential enzyme in the human body that catalyzes the hydrolysis of β -galactosides like lactose. β -Galactosidase is a tetrameric enzyme which consists of four identical subunits [10-12]. Denaturation of the protein in 8M urea results in complete loss of secondary structure, resulting in the formation of unfolded monomer subunits. When the denatured protein is then refolded by diluting it in a renaturing medium (1.4 M urea, 0.1 M sodium phosphate, 1 mM magnesium chloride, 5 mM DTE) , the first step is the formation of folded monomer units, which occurs very quickly. The monomers then associate to form dimers. This is the first rate-limiting step during the refolding process while the structural rearrangement of the dimers is the second rate-limiting

step. The final step which is the association of the dimers to tetramer is again a fast step [13].

1.1.3 Microfluidic devices for protein refolding

Choosing the right solution conditions for protein refolding is an empirical process and is done conventionally using hand-pipeting on a small scale or using robotic systems on a large scale. However, hand-pipeting is labor-intensive while robotic systems are expensive. Microfluidic systems offer several advantages for such combinatorial processes over conventional techniques, like usage of small sample volumes, cost-effectiveness and automation. Several microfluidic devices have been developed by different groups for protein processing and high throughput applications. Zheng et al. [14] have developed a two-phase droplet-based system for protein crystallization application. Although this design is capable of high throughput combinatorial processing [15], it is limited by the dependence of droplet formation on solution viscosity [16]. Reagents like surfactants are not easy to introduce into the aqueous droplet as they tend to stabilize the interface of the two-phase system. Another technique that has gained importance in such applications is the technique of electrowetting-on-dielectric to digitally address droplets [17, 18]. However, the limitations of this system are that the biological samples adhere to the hydrophobic dielectric surface [19]. Also, there are challenges associated with actuating non-aqueous droplets with this system [20]. Other examples of microfluidic devices for protein processing applications include devices made by Hansen et al. [21] that use free interface diffusion for protein crystallization and those made by Kerby et al. [22] that use fluorescent dyes that bind to exposed hydrophobic regions of a protein to make kinetic measurements of protein conformation.

On the other hand, Unger et al. [23] have demonstrated the use of pneumatic valves and pumps in microfluidic device to control flow in an automated fashion and Thorsen et al. [24] have shown the use of a microfluidic multiplexor for large scale integration using minimum number of actuation channels. These systems are independent of the type of solutions used in the device as the actuation is mechanical. We use similar pneumatic valves and pumps in our design of the microfluidic device for combinatorial protein refolding. Also, we use a rotary mixer for mixing the different reagents in our device as it is simple to fabricate and uses very small sample volumes as opposed to staggered-herringbone mixers [25] which involve complex two-step etching process to fabricate and serpentine channels [26] which utilize larger sample volumes.

In **Chapter 2**, we show the use of our PDMS-glass microfluidic device in automating combinatorial protocols. Our device consists of three input channels for selecting reagents, a rotary mixer for mixing the denatured protein with the selected reagents and an output channel to quantify the refolding yield of the protein. We performed specific experiments to show the ability of our device to precisely control sample volumes during injection and to efficiently mix reagents in the rotary mixer. We performed refolding experiments on the protein β -galactosidase and quantified the refolding yield using a fluorometric assay [27]. We showed on-chip quantification of refolding yields using this assay on our microfluidic device, showing the potential for our device to be used in protein refolding applications.

1.2 Development of antibody-based microfluidic biosensors for environmental water sampling

1.2.1 Enteric viruses in environmental water samples

Enteric viruses are viruses that inhabit and replicate in the gastrointestinal tract and cause various gastrointestinal illnesses. Infected humans or host animals shed these virus particles in feces and these are introduced into water bodies through leaking sewage and septic systems and urban run-off systems [28]. These viruses can be transmitted to other individuals and animals by the water route. The United States Environmental Protection Agency (USEPA) maintains a list of waterborne pathogens called the Contaminant Candidate List (CCL) to identify unregulated pathogens for which more information is needed before a regulatory determination can be made. Detection of enteric viruses like adenovirus, calicivirus, enterovirus etc. in environmental water bodies is of particular importance to the EPA as these viruses fall under the CCL. Knowing the type and concentration of these viruses in source water helps to design the right water treatment method to prevent disease outbreak.

1.2.2 Detection of enteric viruses

The detection of enteric viruses in environmental waters requires the ability to process large volumes of water, on the order of hundreds of liters, as these pathogens are present in very concentrations [29]. Conventionally, this is done using electropositive ceramic cartridge filters like 1 MDS and NanoCeram filters, which have high recovery efficiencies and can reduce the sample volumes from hundreds of liters to a few milliliters [30-32]. This concentrated sample is then sent for detection which is

generally done using one of two methods – cell culture methods and molecular methods [33]. In cell culture methods, a monolayer of cells is infected with the viral sample and the number of visible plaques is counted to determine water quality. These methods also give information on the infectivity of viruses [34]. However, they are very time-intensive as they take several days or weeks to culture the cells and also require skilled labor to interpret the results. On the other hand, molecular methods using PCR have become increasingly popular for virus detection as they are not as time-consuming as the cell culture methods. They can also be used for detecting viruses that cannot be grown on established cell lines. Quantitative reverse transcriptase PCR assays using TaqMan probes have been used for the detection of various enteric viruses [35] like hepatitis A virus [36, 37], human adenovirus [38] and Norwalk-like virus [39]. Although these real-time PCR methods exhibit low limits of detection, they are affected by inhibitors (like humic compounds, polysaccharides, metal ions etc.) present in environmental water samples resulting in false negatives. Hence, the samples need to be excessively processed by different methods like dialysis, solvent extraction, ultrafiltration and glass purification, before use in a PCR assay [40, 41].

Integrated cell culture RT-PCR techniques have been developed to overcome the disadvantages associated with conventional cell culture and direct RT-PCR techniques. In these methods, the viruses are made to replicate in cell culture for a short duration followed by PCR amplification. Reynolds et al. have developed such an integrated method for enterovirus detection [42] while adenovirus detection was done by Lee et al. [43]. These methods are less time-consuming than conventional cell culture methods and also give information on virus infectivity. However, this process can decrease the efficiency of detection [44].

Another molecular method used for viral RNA detection is Nucleic Acid Sequence Based Amplification (NASBA), which amplifies RNA at a single temperature of 41°C. This method does not require thermal cycling between two temperatures like in RT-PCR and the time of the overall process is also reduced. NASBA has been used in conjunction with molecular beacons for real-time detection of hepatitis A virus [45] and norovirus [46] in seeded surface water samples. However, synthesis of specific molecular beacon probes for different viruses is expensive. Zaytseva et al. [47] developed a microfluidic biosensor with magnetic bead-based sandwich hybridization system using fluorescent liposomes for Dengue virus RNA detection. This device uses off-chip NASBA for RNA amplification before introducing the sample into the biosensor.

Apart from cell culture and molecular methods, a number of immunobiosensors have been developed for enteric virus detection. An automated portable fiber optic biosensor for MS2 coliphage detection was developed based on a fluorescent sandwich immunoassay [48, 49]. Rossi et al. [50] developed a porous silicon biosensor with antibodies conjugated on nanoporous silicon films for MS2 coliphage detection while Pineda et al. [51] developed a photonic crystal biosensor for the detection of porcine rotavirus. The limits of detection with these biosensors were in the range of 10^4 - 10^9 PFU/ml.

Atomic force microscopy (AFM) and surface-enhanced Raman spectroscopy (SERS) have reported limits of detection of 3×10^6 and 1×10^6 particles/ml for the detection of feline calicivirus (FCV) [52]. However, AFM requires expensive and bulky equipment for detection and depends on the rigidity of viral particles while SERS uses expensive optical systems.

In the portable microfluidic device format, most of the devices that were developed for enteric virus detection use RT-PCR techniques [53-55]. Although these

techniques have the potential to achieve low limits of detection (10 – 100 PFU/ml), they are limited by a number of issues. Apart from the limitation of inhibitors in environmental water samples, miniaturizing PCR has a number of challenges like adhesion of the enzymes to channel walls [56], difficulty in precisely controlling temperatures, sample evaporation and formation of bubbles in channels [57]. Miniaturized NASBA systems do not have temperature cycling issues but these systems require extensive surface pretreatment to avoid adhesion of the three enzymes used during amplification to the channel walls [58, 59].

Table 1.1: Comparison of different techniques for virus detection

Technique	Analyte	Limit of Detection	Low cost/ Portability	Time	Remarks
SERS [52]	FCV	$\sim 1 \times 10^4$ PFU/ml*	Portable but expensive	~20 h assay time	Sensitive and multiplexed analysis
Fiber optic immuno-biosensor [49]	MS2	10^9 PFU/ml	Portable but expensive	10 min assay time	Rapid, automated detection; High limit of detection
Porous silicon immune-biosensor [50]	MS2	2×10^7 PFU/ml	No	~1h assay time	Interfering photo-luminescence issues
Photonic crystal immune-biosensor [51]	Rotavirus	1.8×10^3 PFU/ml	No	30 min assay time	Extensive surface functionalization; single use
Miniaturized integrated RT-PCR devices [53, 55]	Dengue virus [53]	10^2 PFU/ml	Yes	4 h total time	Affected by inhibitors; temperature cycling issues
	Rotavirus [55]	6.4×10^4 copies/ μ l	Yes	1 h RT-PCR time	
Microfluidic immunobiosensor (direct injection)	FCV	2.4×10^6 PFU/ml	Yes	2 h incubation + 20 min on-chip detection	Portable and inexpensive with EC detection
Microfluidic immunobiosensor (preconcentration)	FCV	1.6×10^5 PFU/ml	Yes	2 h incubation + 20 min on-chip detection	Portable and inexpensive with EC detection

*infectious:non-infectious viruses ~ 1:100 for enteroviruses [60]

We have developed an integrated microfluidic biosensor that combines sample preconcentration with antibody-based detection and liposome-based signal amplification for sensitive detection of viruses. This device can be used in electrochemical detection mode by patterning gold interdigitated electrodes in the device and using electrochemical liposomes instead of fluorescent liposomes. The comparison of device performance for our integrated biosensor with various other detection systems is shown Table 1.1. When used in the electrochemical detection mode, our device has the advantages of low cost, portability and quantitative signal read-out.

In **Chapter 3**, we describe the fabrication and characterization of the membrane-based preconcentration system and compare the advantages of this system with existing preconcentration techniques. We performed integrated concentration-detection experiments using fluorescent liposomes for signal amplification and biotin-streptavidin binding as the model system. We performed proof-of-principle experiments using this model system to show the improvement in performance of the device with the inclusion of electrokinetic preconcentration as opposed to a device that does not include any preconcentration.

In **Chapter 4**, we show the detection of Feline Calicivirus (FCV) using the integrated microfluidic device. We chose FCV as a model organism for human enteric viruses [61]. We used capture and probe antibodies for the detection of FCV in a sandwich immunoassay and we used fluorescent liposomes for signal amplification. We performed microtiter plate assays to identify the optimal capture-probe antibody pair for best signals. Using these antibodies, we performed FCV detection experiments with our microfluidic device and estimated a limit of detection of 1.6×10^5 PFU/ml. We then compared the performance of this device with a similar device that does not

include the preconcentration system and found that the integrated device shows a lower limit of detection.

Finally, in **Chapter 5**, we summarized the accomplishments of these two projects and highlighted the path for future work.

1.3 Taylor-Aris dispersion

A common theme in both the protein refolding and virus detection devices is the effect of Taylor-Aris dispersion [62-65], which is a result of the combined effects of axial convection and radial diffusion of the molecules. In the microfluidic device for combinatorial protein refolding, the mixing of reagents in the rotary mixer is due to Taylor-Aris dispersion, which needs to be maximized for efficient mixing. The pump on the rotary mixer adds convection to the flow and helps to overcome the long mixing times characteristic of microfluidic flows which are low Reynolds number and high Peclet number flows. To get an estimate of the relative effects of convection and diffusion in this system, all the relevant geometric parameters of the channels and the diffusivity of dye molecules used in these mixing experiments are listed here. The diameter of the rotary mixer is 2.54 mm, which corresponds to a perimeter of 8 mm. The PDMS microchannels used in these experiments are about 10 μm deep and 100 μm wide. The average velocity of the pressure-driven flow induced by the pump in the channels is 1 mm/s. The diffusivity of the dye molecules in the mixing experiment is on the order of $10^{-10} \text{ m}^2/\text{s}$.

In the absence of convective flow induced by the pump, the only mixing mechanism for dye molecules in the rotary mixer is by axial diffusion. The timescale for this diffusion process scales as L^2/D , where L is the perimeter of the rotary mixer

and D is the diffusivity of the dye molecules. For the values listed above, this timescale is on the order of 1000 min.

When axial convection is now added to this system, the dye molecules follow the parabolic flow profile of the pressure driven flow, with the fast-moving molecules in the center and the slow moving molecules close to the channel walls. The radial diffusion in this system causes the dye molecules to sample both the fast-moving and slow-moving parts of pressure-driven flow, reducing the dispersive effect of the convective flow. The two important parameters governing this flow are the Peclet number $Pe = \bar{u}a/D$ and the length ratio L/a . Here, \bar{u} is the average velocity of pressure-driven flow and a is the depth of the microchannels. For the rotary mixer, $Pe = 100$ and $L/a = 800$. For this regime where $1 \ll Pe \ll L/a$, the averaged 1-D equation for the convection-diffusion problem is given by

$$\frac{\partial \bar{c}}{\partial t} + \bar{u} \frac{\partial \bar{c}}{\partial x} = D_{eff} \frac{\partial^2 \bar{c}}{\partial x^2} \quad (1.1)$$

where the effective diffusivity D_{eff} for a large aspect ratio rectangular channel is given by [66]

$$D_{eff} = D \left(1 + 7.951 \times \frac{Pe^2}{210} \right) \quad (1.2)$$

For $Pe = 100$, the value of D_{eff} is about $380D$. The timescale for mixing with this increased effective diffusivity is now L^2 / D_{eff} which is 2.6 min (380 times lesser than the 1000 min case for pure diffusion). Thus, Taylor-Aris dispersion in the rotary mixer significantly reduces the mixing time of the reagents.

On the other hand, in the microfluidic biosensor for virus detection, Taylor-Aris dispersion needs to be eliminated for efficient concentration and elution. In Figure 1.1, the voltage settings during elution are shown on the microfluidic device.

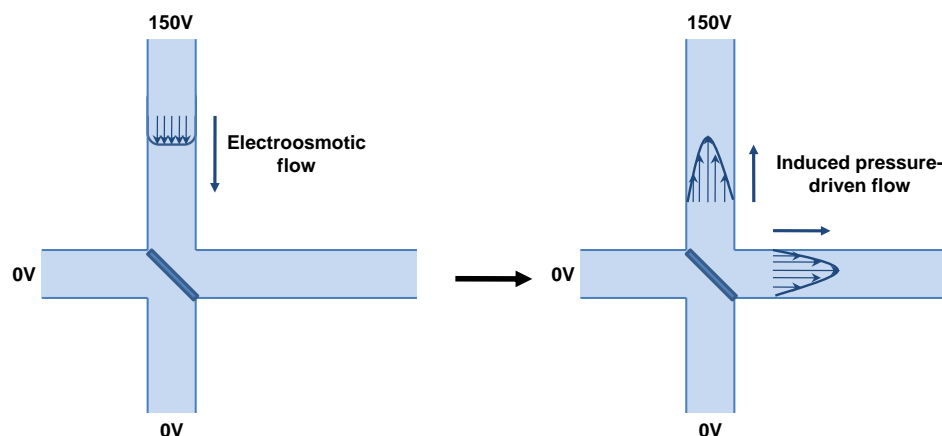


Figure 1.1 (a): Direction of electroosmotic flow in the negatively charged glass microchannel in the integrated microfluidic biosensor when an electric field is applied during elution. (b): The membrane at the junction induces adverse pressure gradients in the channels to satisfy mass conservation, resulting in Poiseuille flow.

For the negatively charged glass channels, the direction of the electroosmotic flow upon applying an electric field is shown in Figure 1.1(a). The presence of the membrane at the junction of the microchannels leads to an adverse pressure gradient being induced in the channels as shown in Figure 1.1(b) to satisfy mass conservation. This pressure-driven flow causes dispersion of the concentrated bolus of analytes during elution. Additionally, external pressure gradients also cause dispersion of the concentrated bolus. This dispersion reduces the local concentration of the liposomes, countering the effect of the concentration system. The electroosmotic flow which is the source of this dispersive pressure-driven flow needs to be eliminated for efficient concentration and elution of analytes. Since the surface charge on the glass channels is

responsible for this electroosmotic flow, the channel walls are coated with linear polyacrylamide which is hydrophilic and uncharged [67]. This polyacrylamide coating reduces the zeta potential of the glass surface to almost zero, thereby eliminating the electroosmotic flow [67].

Hence, in the protein refolding device, the effect of Taylor-Aris dispersion needs to be maximized for efficient mixing of the reagents, while in the virus detection device, this effect needs to be eliminated as it counters the effect of the preconcentration system.

BIBLIOGRAPHY

- [1] D. V. Goeddel, D. G. Kleid, F. Bolivar, H. L. Heyneker, D. G. Yansura, R. Crea, T. Hirose, A. Kraszewski, K. Itakura, and A. D. Riggs, "Expression in Escherichia-Coli of Chemically Synthesized Genes for Human Insulin," *Proc. Natl. Acad. Sci. U. S. A.*, vol. 76, pp. 106-110, 1979.
- [2] L. Gold, "Expression of Heterologous Proteins in Escherichia-Coli," *Methods in Enzymology*, vol. 185, pp. 11-14, 1990.
- [3] S. C. Makrides, "Strategies for achieving high-level expression of genes in Escherichia coli," *Microbiological Reviews*, vol. 60, pp. 512-&, Sep 1996.
- [4] M. M. Carrio and A. Villaverde, "Construction and deconstruction of bacterial inclusion bodies," *Journal of Biotechnology*, vol. 96, pp. 3-12, Jun 2002.
- [5] M. M. Carrio and A. Villaverde, "Protein aggregation as bacterial inclusion bodies is reversible," *Febs Letters*, vol. 489, pp. 29-33, Jan 2001.
- [6] C. B. Anfinsen, "Formation and Stabilization of Protein Structure," *Biochemical Journal*, vol. 128, pp. 737-&, 1972.
- [7] C. N. Pace, B. A. Shirley, M. McNutt, and K. Gajiwala, "Forces contributing to the conformational stability of proteins," *Faseb Journal*, vol. 10, pp. 75-83, Jan 1996.
- [8] G. Zettlmeissl, R. Rudolph, and R. Jaenicke, "Reconstitution of lactic dehydrogenase. Noncovalent aggregation vs. reactivation. 1. Physical properties and kinetics of aggregation," *Biochemistry*, vol. 18, pp. 5567-71, 1979.
- [9] D. L. Hevehan and E. De Bernardez Clark, "Oxidative renaturation of lysozyme at high concentrations," *Biotechnology and Bioengineering*, vol. 54, pp. 221-230, 1997.
- [10] G. R. Craven, E. Steers, Jr., and C. B. Anfinsen, "Purification, composition, and molecular weight of the b-galactosidase of Escherichia coli K12," *Journal of Biological Chemistry*, vol. 240, pp. 2468-77, 1965.
- [11] S. L. Marchesi, E. Steers, Jr., and S. Shifrin, "Purification and characterization of the multiple forms of b-galactosidase of Escherichia coli," *Biochimica et Biophysica Acta, Protein Structure*, vol. 181, pp. 20-34, 1969.
- [12] K. Wallenfels and R. Weil, *Beta-galactosidase*, 3 ed. vol. 7. New York: Academic Press, 1972.

- [13] A. Nichtl, J. Buchner, R. Jaenicke, R. Rudolph, and T. Scheibel, "Folding and association of b-galactosidase," *Journal of Molecular Biology*, vol. 282, pp. 1083-1091, 1998.
- [14] B. Zheng, C. J. Gerdts, and R. F. Ismagilov, "Using nanoliter plugs in microfluidics to facilitate and understand protein crystallization," *Curr. Opin. Struct. Biol.*, vol. 15, pp. 548-555, 2005.
- [15] L. Li, D. Mustafi, Q. Fu, V. Tershko, D. L. Chen, J. D. Tice, and R. F. Ismagilov, "Nanoliter microfluidic hybrid method for simultaneous screening and optimization validated with crystallization of membrane proteins," *Proc. Natl. Acad. Sci. U. S. A.*, vol. 103, pp. 19243-19248, 2006.
- [16] J. D. Tice, A. D. Lyon, and R. F. Ismagilov, "Effects of viscosity on droplet formation and mixing in microfluidic channels," *Anal. Chim. Acta*, vol. 507, pp. 73-77, 2004.
- [17] S. K. Cho, S.-K. Fan, H. Moon, and C.-J. Kim, "Towards digital microfluidic circuits. Creating, transporting, cutting and merging liquid droplets by electrowetting-based actuation," *IEEE Int. Conf. Micro Electro Mech. Syst., Tech. Dig., 15th*, pp. 32-35, 2002.
- [18] R. B. Fair, "Digital microfluidics: is a true lab-on-a-chip possible?," *Microfluid. Nanofluid.*, vol. 3, pp. 245-281, 2007.
- [19] J.-Y. Yoon and R. L. Garrell, "Preventing biomolecular adsorption in electrowetting-based biofluidic chips," *Anal. Chem.*, vol. 75, pp. 5097-5102, 2003.
- [20] D. Chatterjee, B. Hetayothin, A. R. Wheeler, D. J. King, and R. L. Garrell, "Droplet-based microfluidics with nonaqueous solvents and solutions," *Lab Chip*, vol. 6, pp. 199-206, 2006.
- [21] C. L. Hansen, E. Skordalakes, J. M. Berger, and S. R. Quake, "A robust and scalable microfluidic metering method that allows protein crystal growth by free interface diffusion," *Proc. Natl. Acad. Sci. U. S. A.*, vol. 99, pp. 16531-16536, Dec 2002.
- [22] M. B. Kerby, J. Lee, J. Ziperstein, and A. Tripathi, "Kinetic Measurements of Protein Conformation in a Microchip," *Biotechnology Progress*, vol. 22, pp. 1416-1425, 2006.
- [23] M. A. Unger, H.-P. Chou, T. Thorsen, A. Scherer, and S. R. Quake, "Monolithic microfabricated valves and pumps by multilayer soft lithography," *Science (Washington, D. C.)*, vol. 288, pp. 113-116, 2000.

- [24] T. Thorsen, S. J. Maerkl, and S. R. Quake, "Microfluidic Large-Scale Integration," *Science (Washington, DC, United States)*, vol. 298, pp. 580-584, 2002.
- [25] A. D. Stroock, S. K. W. Dertinger, A. Ajdari, I. Mezit, H. A. Stone, and G. M. Whitesides, "Chaotic mixer for microchannels," *Science (Washington, DC, U. S.)*, vol. 295, pp. 647-651, 2002.
- [26] R. H. Liu, M. A. Stremler, K. V. Sharp, M. G. Olsen, J. G. Santiago, R. J. Adrian, H. Aref, and D. J. Beebe, "Passive mixing in a three-dimensional serpentine microchannel," *Journal of Microelectromechanical Systems*, vol. 9, pp. 190-197, 2000.
- [27] B. Rotman, J. A. Zderic, and M. Edelstein, "Fluorogenic substrates for b-D-galactosidases and phosphatases derived from fluorescein (3,6-dihydroxyfluoran) and its mono-methyl ether," *Proceedings of the National Academy of Sciences of the United States of America*, vol. 50, pp. 1-6, 1963.
- [28] T.-T. Fong and E. K. Lipp, "Enteric viruses of humans and animals in aquatic environments: Health risks, detection, and potential water quality assessment tools," *Microbiol. Mol. Biol. Rev.*, vol. 69, pp. 357-371, 2005.
- [29] A. Bosch, S. Guix, D. Sano, and R. M. Pinto, "New tools for the study and direct surveillance of viral pathogens in water," *Curr. Opin. Biotechnol.*, vol. 19, pp. 295-301, 2008.
- [30] M. D. Sobsey and J. S. Glass, "Poliovirus concentration from tap water with electropositive adsorbent filters," *Appl Environ Microbiol*, vol. 40, pp. 201-10, 1980.
- [31] M. R. Karim, E. R. Rhodes, N. Brinkman, L. Wymer, and G. S. Fout, "New electropositive filter for concentrating enteroviruses and noroviruses from large volumes of water," *Appl. Environ. Microbiol.*, vol. 75, pp. 2393-2399, 2009.
- [32] C. D. Gibbons, R. A. Rodriguez, L. Tallon, and M. D. Sobsey, "Evaluation of positively charged alumina nanofibre cartridge filters for the primary concentration of noroviruses, adenoviruses and male-specific coliphages from seawater," *J. Appl. Microbiol.*, vol. 109, pp. 635-641, 2010.
- [33] T. G. Metcalf, J. L. Melnick, and M. K. Estes, "Environmental virology: from detection of virus in sewage and water by isolation to identification by molecular biology - a trip of over 50 years," *Annu. Rev. Microbiol.*, vol. 49, pp. 461-87, 1995.

- [34] R. A. Rodriguez, I. L. Pepper, and C. P. Gerba, "Application of PCR-Based Methods To Assess the Infectivity of Enteric Viruses in Environmental Samples," *Appl. Environ. Microbiol.*, vol. 75, pp. 297-307, Jan 2009.
- [35] D. Pusch, D. Y. Oh, S. Wolf, R. Dumke, U. Schroter-Bobsin, M. Hohne, I. Roske, and E. Schreier, "Detection of enteric viruses and bacterial indicators in German environmental waters," *Archives of Virology*, vol. 150, pp. 929-947, May 2005.
- [36] M. I. Costafreda, A. Bosch, and R. M. Pinto, "Development, evaluation, and standardization of a real-time TaqMan reverse transcription-PCR assay for quantification of hepatitis A virus in clinical and shellfish samples," *Appl. Environ. Microbiol.*, vol. 72, pp. 3846-3855, Jun 2006.
- [37] G. Sanchez, A. Bosch, and R. M. Pinto, "Hepatitis A virus detection in food: current and future prospects," *Letters in Applied Microbiology*, vol. 45, pp. 1-5, Jul 2007.
- [38] N. Jothikumar, T. L. Cromeans, V. R. Hill, X. Y. Lu, M. D. Sobsey, and D. D. Erdman, "Quantitative real-time PCR assays for detection of human adenoviruses and identification of serotypes 40 and 41," *Appl. Environ. Microbiol.*, vol. 71, pp. 3131-3136, Jun 2005.
- [39] T. Kageyama, S. Kojima, M. Shinohara, K. Uchida, S. Fukushi, F. B. Hoshino, N. Takeda, and K. Katayama, "Broadly reactive and highly sensitive assay for Norwalk-like viruses based on real-time quantitative reverse transcription-PCR," *Journal of Clinical Microbiology*, vol. 41, pp. 1548-1557, Apr 2003.
- [40] Y. S. C. Shieh, D. Wait, L. Tai, and M. D. Sobsey, "Methods to remove inhibitors in sewage and other fecal wastes for enterovirus detection by the polymerase chain reaction," *J. Virol. Methods*, vol. 54, pp. 51-66, 1995.
- [41] M. M. Ijzerman, D. R. Dahling, and G. S. Fout, "A method to remove environmental inhibitors prior to the detection of waterborne enteric viruses by reverse transcription-polymerase chain reaction," *J. Virol. Methods*, vol. 63, pp. 145-153, 1997.
- [42] K. A. Reynolds, C. P. Gerba, and I. L. Pepper, "Detection of infectious enteroviruses by an integrated cell culture PCR procedure," *Appl. Environ. Microbiol.*, vol. 62, pp. 1424-1427, Apr 1996.
- [43] S. H. Lee and S. J. Kim, "Detection of infectious enteroviruses and adenoviruses in tap water in urban areas in Korea," *Water Research*, vol. 36, pp. 248-256, Jan 2002.

- [44] P. Wyn-Jones, "The Detection of Waterborne Viruses," in *Human Viruses in Water*, vol. 17, A. Bosch, Ed. Amsterdam, The Netherlands: Elsevier, 2007, pp. 177-204.
- [45] K. H. A. El Galil, M. A. El Sokkary, S. M. Kheira, A. M. Salazar, M. V. Yates, W. Chen, and A. Mulchandani, "Real-time nucleic acid sequence-based amplification assay for detection of hepatitis A virus," *Appl. Environ. Microbiol.*, vol. 71, pp. 7113-7116, Nov 2005.
- [46] S. A. Rutjes, H. van den Berg, W. J. Lodder, and A. M. D. Husman, "Real-time detection of noroviruses in surface water by use of a broadly reactive nucleic acid sequence-based amplification assay," *Appl. Environ. Microbiol.*, vol. 72, pp. 5349-5358, Aug 2006.
- [47] N. V. Zaytseva, R. A. Montagna, and A. J. Baeumner, "Microfluidic biosensor for the serotype-specific detection of Dengue virus RNA," *Anal. Chem.*, vol. 77, pp. 7520-7527, Dec 2005.
- [48] G. P. Anderson, K. D. King, K. L. Gaffney, and L. H. Johnson, "Multi-analyte interrogation using the fiber optic biosensor," *Biosens. Bioelectron.*, vol. 14, pp. 771-777, Jan 2000.
- [49] K. D. King, J. M. Vanniere, J. L. Leblanc, K. E. Bullock, and G. P. Anderson, "Automated fiber optic biosensor for multiplexed immunoassays," *Environmental Science & Technology*, vol. 34, pp. 2845-2850, Jul 2000.
- [50] A. M. Rossi, L. Wang, V. Reipa, and T. E. Murphy, "Porous silicon biosensor for detection of viruses," *Biosens. Bioelectron.*, vol. 23, pp. 741-745, Dec 2007.
- [51] M. F. Pineda, L. L. Y. Chan, T. Kuhlenschmidt, C. J. Choi, M. Kuhlenschmidt, and B. T. Cunningham, "Rapid Specific and Label-Free Detection of Porcine Rotavirus Using Photonic Crystal Biosensors," *Ieee Sensors Journal*, vol. 9, pp. 470-477, Apr 2009.
- [52] M. D. Porter, J. D. Driskell, K. M. Kwarta, R. J. Lipert, J. D. Neill, and J. F. Ridpath, "Detection of Viruses: Atomic Force Microscopy and Surface Enhanced Raman Spectroscopy," *Developments in Biologicals*, vol. 126, pp. 31-39, 2006.
- [53] K.-Y. Lien, W.-C. Lee, H.-Y. Lei, and G.-B. Lee, "Integrated reverse transcription polymerase chain reaction systems for virus detection," *Biosens. Bioelectron.*, vol. 22, pp. 1739-1748, 2007.
- [54] W.-C. Lee, K.-Y. Lien, G.-B. Lee, and H.-Y. Lei, "An integrated microfluidic system using magnetic beads for virus detection," *Diagn. Microbiol. Infect. Dis.*, vol. 60, pp. 51-58, 2008.

- [55] Y. Li, C. Zhang, and D. Xing, "Fast identification of foodborne pathogenic viruses using continuous-flow reverse transcription-PCR with fluorescence detection," *Microfluid. Nanofluid.*, vol. 10, pp. 367-380, 2011.
- [56] C. Zhang, J. Xu, W. Ma, and W. Zheng, "PCR microfluidic devices for DNA amplification," *Biotechnol. Adv.*, vol. 24, pp. 243-284, 2006.
- [57] C. Zhang and D. Xing, "Miniaturized PCR chips for nucleic acid amplification and analysis: latest advances and future trends," *Nucleic Acids Res.*, vol. 35, pp. 4223-4237, 2007.
- [58] I. K. Dimov, J. L. Garcia-Cordero, J. O'Grady, C. R. Poulsen, C. Viguier, L. Kent, P. Daly, B. Lincoln, M. Maher, R. O'Kennedy, T. J. Smith, A. J. Ricco, and L. P. Lee, "Integrated microfluidic tmRNA purification and real-time NASBA device for molecular diagnostics," *Lab Chip*, vol. 8, pp. 2071-2078, 2008.
- [59] A. Gulliksen, L. Solli, F. Karlsen, H. Rogne, E. Hovig, T. Nordstrom, and R. Sirevag, "Real-time nucleic acid sequence-based amplification in nanoliter volumes," *Anal. Chem.*, vol. 76, pp. 9-14, Jan 2004.
- [60] H. Kopecka, S. Dubrou, J. Prevot, J. Marechal, and J. M. Lopez-Pila, "Detection of naturally occurring enteroviruses in waters by reverse transcription, polymerase chain reaction, and hybridization," *Appl. Environ. Microbiol.*, vol. 59, pp. 1213-19, 1993.
- [61] J. A. Tree, M. R. Adams, and D. N. Lees, "Disinfection of feline calicivirus (a surrogate for Norovirus) in wastewaters," *J. Appl. Microbiol.*, vol. 98, pp. 155-162, 2005.
- [62] G. Taylor, "Dispersion of Soluble Matter in Solvent Flowing Slowly through a Tube," *Proceedings of the Royal Society of London Series a-Mathematical and Physical Sciences*, vol. 219, pp. 186-203, 1953.
- [63] G. Taylor, "Conditions under Which Dispersion of a Solute in a Stream of Solvent Can Be Used to Measure Molecular Diffusion," *Proceedings of the Royal Society of London Series a-Mathematical and Physical Sciences*, vol. 225, pp. 473-477, 1954.
- [64] R. Aris, "On the Dispersion of a Solute in a Fluid Flowing through a Tube," *Proceedings of the Royal Society of London Series a-Mathematical and Physical Sciences*, vol. 235, pp. 67-77, 1956.
- [65] R. Aris, "On the Dispersion of a Solute by Diffusion, Convection and Exchange between Phases," *Proceedings of the Royal Society of London Series a-Mathematical and Physical Sciences*, vol. 252, pp. 538-550, 1959.

- [66] H. Brenner and D. A. Edwards, *Macrotransport Processes*. Boston: Butterworth-Heinemann, 1993.
- [67] B. J. Kirby, A. R. Wheeler, R. N. Zare, J. A. Fruetel, and T. J. Shepodd, "Programmable modification of cell adhesion and zeta potential in silica microchips," *Lab Chip*, vol. 3, pp. 5-10, 2003.

CHAPTER 2

REFOLDING OF β -GALACTOSIDASE: MICROFLUIDIC DEVICE FOR REAGENT METERING AND MIXING AND QUANTIFICATION OF REFOLDING YIELD

2.1 *Abstract*

We have developed a device that uses microfluidic valves and pumps to meter reagents for subsequent mixing with application to refolding of the protein β -galactosidase. The microfluidic approach offers the potential advantages of automation, cost-effectiveness, compatibility with optical detection, and reduction in sample volumes as opposed to conventional techniques of hand-pipeting or using robotic systems. The device is a multi-layered Poly(dimethylsiloxane) (PDMS) on glass device with automated controls for reagent aliquoting and mixing. Refolding experiments have been performed off-chip using existing protocols on the protein β -galactosidase and the refolding yield has been quantified on-chip using fluorescein di- β -D-galactopyranoside (FDG), a caged-fluorescent molecule. This work provides the potential to reduce the cost of drug discovery and realization of protein pharmaceuticals.

2.2 *Introduction*

Protein refolding has been a bottleneck in the production of biopharmaceuticals on a large scale. Synthesis of recombinant proteins in the biopharmaceutical industry uses

bacterial systems like *E. coli* as hosts. To over-express the production of recombinant proteins, promoters are used to induce genetically modified bacteria. This over-expression leads to the formation of misfolded protein aggregates called inclusion bodies [1] The process of refolding involves the conversion of these non-functional protein aggregates to their functional native state. However, in most cases, the solution conditions to properly refold proteins are not known a priori. Determination of these solution conditions is a highly empirical process.

The process of finding the reagents and buffers to properly refold proteins has been conventionally done by hand-pipeting, which is a highly time and labor-intensive process, or using robotic systems, which are very expensive. In either case, proteins are mixed combinatorially with various reagents on a 96-well plate, thus requiring expensive proteins and reagents on the order of several milliliters. The refolding yield is then quantified using various techniques like immuno affinity [2, 3] or spectroscopic methods [4].

The microfluidic approach has many potential advantages compared to conventional techniques. The sample volumes used in microfluidic devices are on the order of nanoliters as opposed to milliliters used in the conventional methods, resulting in a million-fold volume reduction. Additionally, no expensive robotic control is involved for automation of fluid handling. Both these factors contribute to the cost-effectiveness of the microfluidic device.

Kinetic measurements of protein conformation during unfolding and refolding are important in validating models for the folding process. Different methods are employed on microfluidic platforms to study the intermediate protein states like fluorescent dyes that bind to exposed hydrophobic regions of partially folded proteins [5] or techniques like small-angle x-ray scattering [6] and terahertz spectroscopy [7]. Our device is compatible with on-chip optical detection, which gives the potential for

real-time monitoring of these kinetic intermediates using the various techniques mentioned above.

The upcoming sections are organized as follows: First, details of refolding of the protein β -galactosidase are discussed. Next, materials and methods to fabricate the device and implement the refolding protocol are discussed. The next section deals with device design to achieve refolding on-chip. The last few sections present the results, discussion and conclusion.

2.3 β -Galactosidase refolding

Refolding experiments are performed on the protein β -galactosidase, which is an essential enzyme in the human body that catalyzes the hydrolysis of β -galactosides like lactose into monosaccharides [8]. Commercial preparations of the enzyme are used in the preparation of lactose-free products and tablets to cater to the large lactose intolerant population. Apart from its biological activity, the enzyme has gained importance in molecular biology as a reporter protein [9, 10]. β -galactosidase is encoded by the lacZ gene of the lac operon in E.coli. Activity of a promoter that is fused to the lacZ gene can thus be detected by measuring the levels of β -galactosidase [9, 10].

The structural and enzymatic properties of the enzyme have been well characterized [10-16]. It is one of the largest tetrameric enzymes known at present, with a total of 1023 amino acids [17, 18]. Early studies on the protein showed that it can be denatured in the presence of high concentrations of urea [16, 19-21] while the folding pathway of the protein was studied by Nichtl et al. in 1998.

The denaturing protocol for the protein involves solubilizing in a buffer solution containing 8M urea [19]. The solubilized protein along with the denaturants is then diluted in a renaturing medium which mainly contains low concentration denaturing agent (1.4M urea) and Mg^{2+} ions that aid refolding [19].

In this paper, we show the potential of our microfluidic device in automating fluid handling for performing protein refolding trials. On-chip refolding yield measurements are performed using a fluorometric assay on the protein β -galactosidase.

2.4 Materials and methods

2.4.1 Reagents

Urea, dithioerythritol (DTE), sodium phosphate, 1,1,2,2 tetrahydro – perfluorooctyltrichlorosilane, β -galactosidase from *E. coli* and dimethyl sulfoxide (DMSO) were from Sigma Aldrich (St. Louis, MO). Ethylene diamine tetraacetic acid (EDTA) and magnesium chloride were from EMD chemicals (Gibbstown, NJ). Fluorescein di- β -D-galactopyranoside (FDG) was from Invitrogen (Carlsbad, CA).

2.4.2 Device fabrication

The microfluidic device was fabricated using replica molding of poly(dimethylsiloxane) on microfabricated molds [22]. Device geometries were defined using L-Edit CAD software (Tanner Research). Two mask patterns were created using a GCA/Mann 3600F Optical Pattern Generator – one for the ‘flow

channels', the channels through which the various reagents flow and the other for the 'control channels', the channels through which pressurized air flows. The silicon wafer used as a master for the flow channels was coated with a 9 μm thick layer of SPR 220-7.0 photoresist and the wafer used for the control channels was coated with a 15 μm thick layer of SU-8 2010 photoresist. The wafers were then exposed using the corresponding masks using an EV 620 alignment tool. The SPR resist was developed using a 300MIF resist developer and the channels were rounded by reflowing at 120°C for two minutes. The SU-8 resist was developed using SU-8 developer and rinsed with isopropyl alcohol and deionized water. Both the masters were surface treated by placing 30 μl of 1,1,2,2 tetrahydro – perfluorooctyltrichlorosilane in a vial along with the masters in vacuum for two hours [23].

The PDMS layer containing the flow channels was about 5 mm thick and was prepared by mixing the two-part silicone elastomer (Dow Corning Sylgard® 184) in 5:1 ratio and curing it over the flow master. The layer containing the control channels was about 17 μm thick and was prepared by mixing the elastomer in 20:1 ratio and spin coating the control master at 1750 rpm for 60s. The two PDMS layers were activated in the plasma cleaner and bonded together [23]. The two layered device was then bonded to a glass slide by a similar procedure. Tygon tubes were attached to the reservoirs of the control and flow channels. The control lines were connected to eight-channel manifolds that were controlled through a BOB3 breakout controller board (Fluidigm, San Francisco, CA). The opening/closing of valves and frequency of actuation of the pumps were controlled using an NI-DAQ card (NI 6533 - National Instruments) connected to the breakout board. The control interface was created using LabView program that allows for automation of the control process.

2.4.3 Device preparation

In order to prevent the adhesion of proteins and other particles to the PDMS channels, the channel walls were coated with a layer of bovine serum albumin (BSA) which preferentially adheres to the channels. The channels were thoroughly purged with deionized water before performing multiple refolding trials. Implementing the refolding protocol on-chip requires long incubation times which may result in the evaporation of the reagents through PDMS. This can be prevented by placing the device in a water bath during long incubation hours.

2.4.4 Denaturing and refolding protocols

The denaturing and refolding protocols listed here were performed off-chip using standard pipeting techniques. β -Galactosidase was denatured by incubating 35 μ g/ml of the protein in 8M urea, 1mM ethylene diamine tetraacetic acid (EDTA), 10 mM dithioerythritol (DTE), 0.1 M sodium phosphate (pH 7.5) at 25°C for 2 hours.

Refolding experiments were carried out by diluting the solubilized protein along with the denaturants 1:12 in a refolding medium containing 0.1M sodium phosphate, 1mM magnesium chloride, 5 mM DTE, 1.4M urea (pH 7.5). The protein was incubated in the refolding medium at 10°C for 30 minutes and further incubated at 20 °C for 12 hours [19].

2.4.5 Activity assay

The activity of β -galactosidase was determined by a fluorometric assay using fluorescein di- β -D-galactopyranoside (FDG) as the substrate [24, 25]. Nonfluorescent

FDG was sequentially hydrolyzed by the enzyme, first to fluorescein monogalactosidase (FMG) and then to fluorescein, which is highly fluorescent. A 20mM stock solution of FDG was prepared by dissolving 5 mg in 8:1:1 H₂O/DMSO/ethanol solution. The assay was performed off-chip in a well plate by mixing equal volumes of refolded protein and FDG diluted to 0.2 mM solution, allowing 2 hours of incubation at room temperature.

2.4.6 Fluorescence measurements

The denatured and refolded protein samples were mixed with the diluted FDG solution off-chip and were allowed to incubate for 2 hours. The incubated mixtures were then introduced individually into the microchannels of the device. The emitted fluorescence was observed in the microchannel region using a Nikon TE2000U inverted fluorescence microscope with fixed excitation. Images were obtained using a Q-Imaging Retiga camera and Phylum software. Image analysis was carried out in MATLAB.

2.4.7 Image processing

The volume injection rate of fluid in a flow channel was determined by monitoring the interface between water and dye and estimating the elapsed time for the dye-water interface to move a given distance using image processing tools in MATLAB. The mixing time of reagents in the annular mixer was estimated by visual inspection by filling about half the annulus with water and the other half with dye and actuating the peristaltic pump on the annulus.

2.5 *Device design*

The microfluidic device was designed to enable automated fluidic handling of reagents. This requires precise control over the choice and the amount of the various reagents which was achieved using a design consisting of two layers of poly(dimethylsiloxane) (PDMS) on glass [22]. PDMS is a popular elastomeric material that has been used for a number of microfluidic handling applications [26-28]. A schematic of the channel layout is shown in Figure 2.1. The protein solution and the various reagents flow through the microchannels in the top thick PDMS layer. The channels in this layer called the ‘flow channels’ are 90 μm wide. Pressurized air was passed through the microchannels in the thin PDMS layer to control the flow of reagents in the flow layer. The channels in this thin layer, which is sandwiched between the top thick PDMS layer and the glass slide, are called ‘control channels’ and these channels are 120 μm wide. Each flow channel was equipped with a valve and pump to control the choice and amount of the reagents flowing through it. The chosen reagents were then mixed with the protein solution in the annular mixer [29] which has a radius of 1270 μm . The output was the protein refolded to different degrees depending on the solution conditions. The process was automated using a proprietary circuit and a LabView program. A picture of the device connected to a valve manifold is shown in Figure 2.2. The degree of refolding was then quantified using a fluorometric assay [24, 25].

The preliminary design of the device contains three input channels for conducting refolding trials. Subsequent versions can be expanded by incorporating multiple input channels for implementing complex combinatorial refolding protocols.

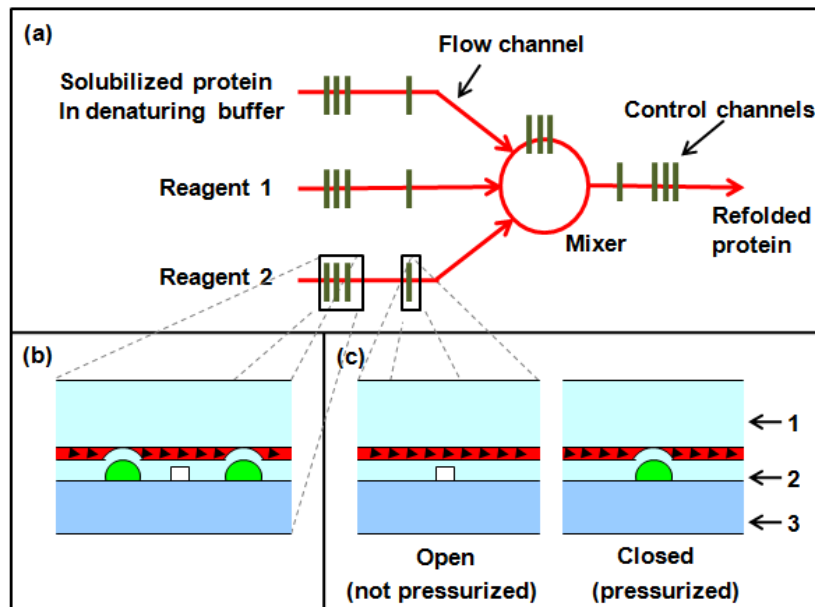


Figure 2.1 (a): Schematic of the channel layout with the red lines representing flow channels and the green lines representing control channels. (b): Peristaltic pump action in the device. (c): Valve action in the device.

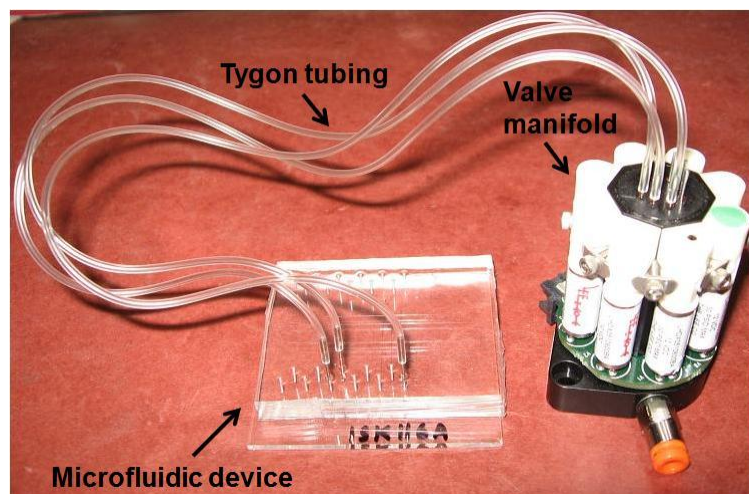


Figure 2.2: Microfluidic device integrated to an eight-valve manifold through tygon tubing. The size of the glass slide to which the PDMS layers are bonded is 2"x3".

2.6 Results

Results described in this section are as follows: (1) The device was characterized by determining the optimum pumping frequency and mixing time of reagents in the annulus. (2) The refolding protocol and the fluorometric assay were optimized off-chip for best on-chip signal intensity. (3) The fluorescence intensity was then calibrated as a function of β -galactosidase concentration in a PDMS microchannel. (4) Finally, the active protein content in denatured and refolded protein samples was quantified on-chip using the obtained calibration curve.

2.6.1 Determination of optimum pumping frequency

Fluid actuation was characterized to facilitate reagent metering. The flow rate of the fluid in the channel depends on the frequency of actuation of the peristaltic pump on the flow channel [22]. The peristaltic actuation of the control channels creates a positive displacement which results in fluid flow. The volume injection rate was calibrated against the frequency of actuation of the control channels as shown in Figure 2.3. The volume injection rate was determined using techniques described in section 2.4.7. The flow rate is maximum at a pumping frequency of about 10 Hz, beyond which the valve opening/closing is incomplete.

2.6.2 Reagent mixing in the annulus

The mixing time of reagents in the annulus was estimated by performing dye-water mixing experiments. The water and dye were introduced through the input channels into the mixing ring and the valves on all the channels connected to the ring were

closed. The pump on the ring was then actuated which resulted in the mixing of the water and dye solutions. Snapshots of the device during mixing are shown in Figure 2.4. The mixing time was estimated as 45s using techniques described in section 2.4.7. The pump on the annulus is operated at 10 Hz actuation frequency.

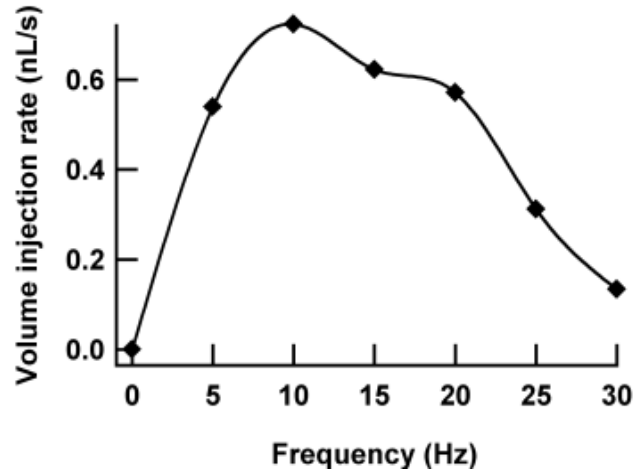


Figure 2.3: Volume injection rate in a flow channel plotted against the frequency of actuation of the control channels.

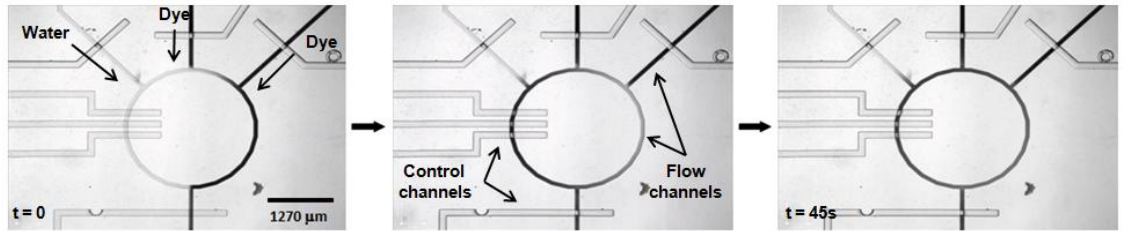


Figure 2.4: Snapshots of the device at different times during mixing. Complete mixing is accomplished in about 45s. The flow rate of the fluid in the mixing ring upon actuation of the peristaltic pump is 1.07 nl/s.

2.6.3 Determination of optimum FDG incubation time

As described in section 2.4.5, nonfluorescent FDG is used as the substrate for measuring β -galactosidase activity. β -Galactosidase sequentially hydrolyzes FDG first to FMG (fluorescein monogalactoside) which is not fluorescent and then to fluorescein which is highly fluorescent. The turnover rate for the hydrolysis of FDG to FMG is relatively slow ($1.9 \mu\text{mol min}^{-1} \text{mg}^{-1}$) compared to the rate of conversion of FMG to fluorescein ($22.7 \mu\text{mol min}^{-1} \text{mg}^{-1}$) [30]. This multistep hydrolysis results in a delay in the production of fluorescence. Hence for obtaining sensitive measurements, very short incubation times, typically less than 10 min, should be avoided.

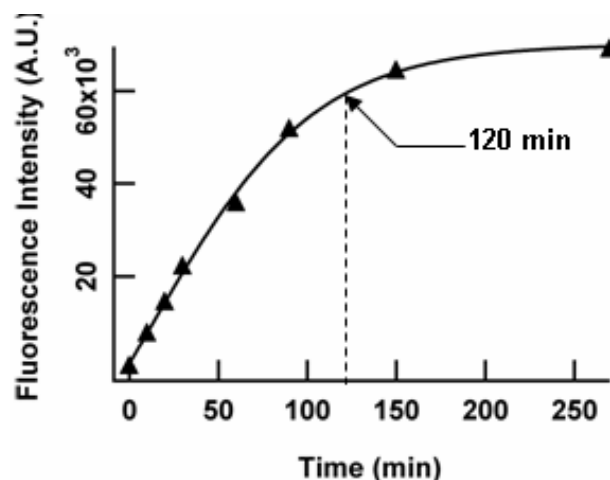


Figure 2.5: Fluorescence signal as a function of FDG – β Galactosidase incubation time. The line is a sigmoidal curve fit to the data.

The fluorometric activity assay for quantifying the activity of β -galactosidase was performed with different FDG incubation times ranging from 0 through 270 minutes. The incubation was performed off-chip at room temperature. Active β -galactosidase at a very low concentration of 0.02 units/ml was used for these trials. A plot of the fluorescence signal intensity as a function of the incubation time is shown

in Figure 2.5. Increasing the reaction time results in an overall increase in signal. However, the curve describing the increasing trend in fluorescence begins to flatten at long incubation times (greater than 90 min.). All subsequent activity measurements were performed with an FDG incubation time of 120 min, based on the FDG - β -galactosidase assay protocol in Huang 1991.

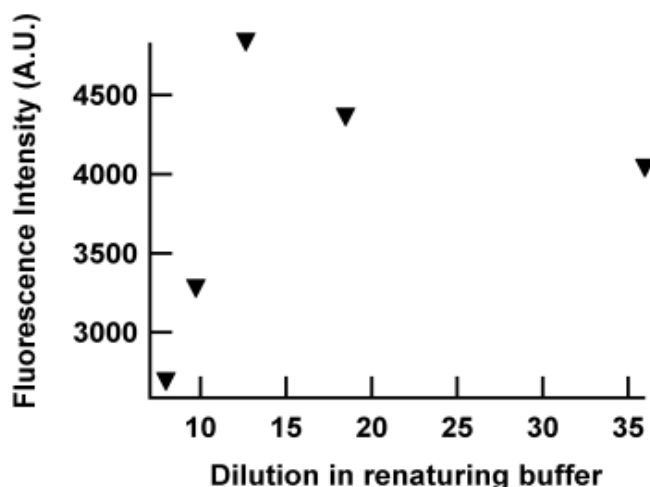


Figure 2.6: Fluorescence signal intensity plotted as a function of dilution of the solubilized protein in the refolding buffer.

2.6.4 Determination of optimum dilution ratio

The refolding protocol was optimized off-chip by performing experiments with different dilutions of the solubilized protein in the renaturing buffer. The protein was denatured following the same protocol described in the materials and methods section. During refolding, the solubilized protein was diluted in different ratios in the renaturing buffer: 8, 10, 12, 18, and 36. FDG was added to these samples and incubated for 120 min. The fluorescence signal intensity was plotted as a function of dilution as shown in Figure 2.6. A dilution ratio of 12 results in the maximum fluorescence signal and this ratio was used in all subsequent refolding experiments.

2.6.5 Calibration of fluorescence intensity in a PDMS microchannel

In order to quantify the refolding yield of β -galactosidase on-chip, the fluorescence intensity of the FDG – protein mixture was calibrated in the PDMS microchannel as a function of β -galactosidase concentration as shown in Figure 2.7. Active β -galactosidase was used for these measurements with concentrations corresponding to 2.5, 5, 10, 20, and 40 units/ml. The fluorescence intensity was calculated by processing fluorescent micrographs of the channel. The flattening of the curve observed at high protein concentrations is due to pixel saturation.

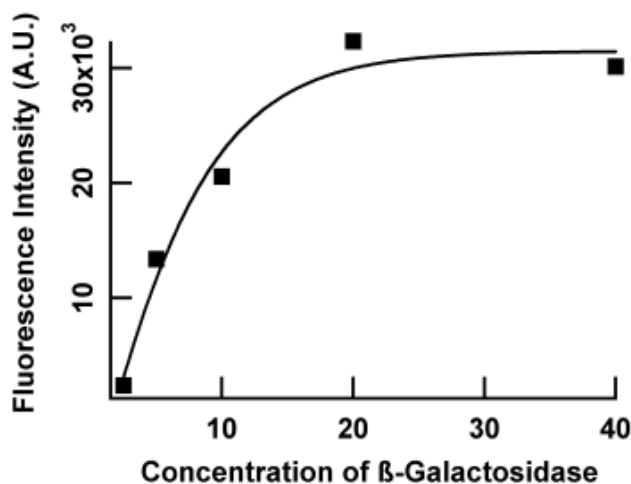


Figure 2.7: Calibration curve of β -galactosidase concentration versus fluorescence intensity in a PDMS microchannel. The intensity is calculated by processing fluorescent micrographs of the channel.

2.6.6 Quantifying active protein content in denatured and refolded samples on-chip

Multiple denaturing and refolding experiments were performed with β -galactosidase as per the optimized protocols described in the materials and methods section. The

refolding yield was determined using the fluorometric assay by quantifying the fluorescence intensity of denatured and refolded samples in the microchannel using image processing techniques. The micrographs of the device filled with denatured and refolded protein samples were used in conjunction with the calibration curve to estimate the refolding yield as $36.84\% \pm 20.96\%$ as shown in the bar graph in Figure 2.8.

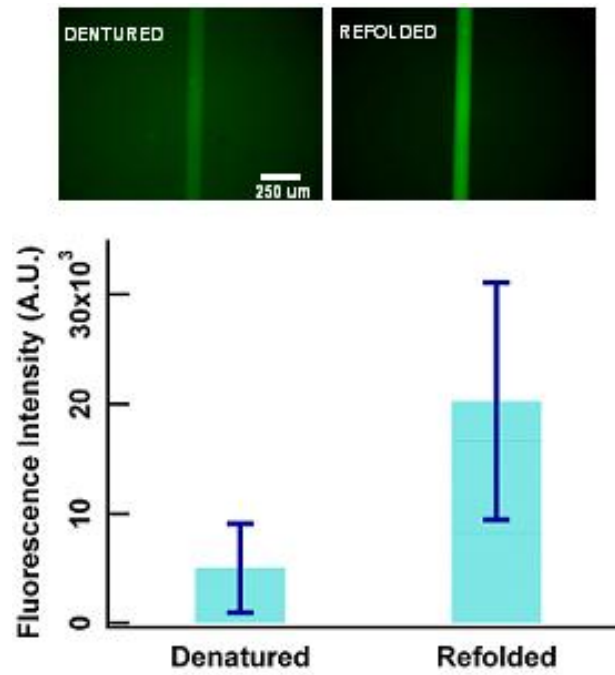


Figure 2.8: Micrograph of device filled with denatured and refolded β -galactosidase samples. The protein samples are incubated with FDG off-chip and introduced into the microchannels to quantify the yield. The bar graph shows the fluorescence intensities of the denatured and refolded samples (n=3).

2.7 Discussion

The refolding yields obtained in these trials are on the order of $36.84\% \pm 20.96\%$, comparable to the yields achieved in the existing literature which were on the order of

35 – 40% [19]. While these yields are still relatively low compared to the percentage refolding that has been achieved for other proteins such as lysozyme [31], these results demonstrate that on-chip reagent mixing characterization can be brought to bear on refolding problems.

The main challenge in refolding proteins is the competing kinetics between aggregation and refolding [32]. The aggregated states correspond to local minima in the protein energy landscape [33]. These metastable states encountered in the folding pathways result in the formation of inclusion bodies. The most common technique to overcome aggregation is to use very dilute solutions of protein during refolding. However, dilute solutions are not cost-effective. Hence recent refolding trials have resorted to the use of small concentrations of denaturants and other reagents that aid refolding by minimizing aggregation. These synthetic reagents which comprise different types of surfactants, salts and sugars that aid in refolding are called artificial chaperones [31]. By combinatorially choosing these artificial chaperones using our microfluidic device, the refolding yield can be improved.

Another technique to improve the refolding yield is to add molecular chaperones like GroEL to the renaturing buffer, that aid in folding by encapsulating individual proteins, thereby preventing aggregation [34]. It has been shown that the presence of GroEL results in a two-fold increase of the in-vitro refolding yield of β -galactosidase [34].

As mentioned earlier, our microfluidic approach provides a cost-effective way to implement refolding protocols because the volumes of reagents used in the trials are on the order of nanoliters and automation does not require the use of expensive robotic systems. Since the device is optically clear, it is compatible with on-chip detection of protein intermediates. The process of scaling up to implement complex combinatorial protocols involves the fabrication of multiple refolding mixers on a single chip to

parallelize the reactions. It has been shown that microfluidic large-scale integration using multiplexors allows control over a large network of fluidic channels with minimal number of inputs [27].

2.8 Conclusion

We have shown the potential of our microfluidic approach in automating fluid handling and have evaluated protein refolding protocols with on-chip measurements. We have demonstrated the capability of our device in controlling reagent metering and mixing by performing experiments with dye-water solutions and mixing them in an annular mixer in an automated fashion. We have optimized a refolding protocol and fluorometric assay off-chip for best on-chip signal intensity, and shown that denatured and refolded samples of the protein β -galactosidase can be quantified on-chip using a fluorescence based assay.

2.9 Acknowledgements

The authors would like to acknowledge useful discussions with Prof. David Putnam and the lab assistance of Mike Arszman, Dino Castellucci and Prashant Sundar.

BIBLIOGRAPHY

- [1] D. C. Williams, R. M. Van Frank, W. L. Muth, and J. P. Burnett, "Cytoplasmic inclusion bodies in *Escherichia coli* producing biosynthetic human insulin proteins," *Science (Washington, DC, United States)*, vol. 215, pp. 687-9, 1982.
- [2] J. M. Teale and D. C. Benjamin, "Antibody as an immunological probe for studying the refolding of bovine serum albumin. II. Evidence for the independent refolding of the domains of the molecule," *Journal of Biological Chemistry*, vol. 251, pp. 4609-15, 1976.
- [3] J. M. Teale and D. C. Benjamin, "Antibody as an immunological probe for studying the refolding of bovine serum albumin. I. The catalysis of reoxidation of reduced bovine serum albumin by glutathione and a disulfide interchange enzyme," *Journal of Biological Chemistry*, vol. 251, pp. 4603-8, 1976.
- [4] J. T. Pelton and L. R. McLean, "Spectroscopic Methods for Analysis of Protein Secondary Structure," *Analytical Biochemistry*, vol. 277, pp. 167-176, 2000.
- [5] M. B. Kerby, J. Lee, J. Ziperstein, and A. Tripathi, "Kinetic Measurements of Protein Conformation in a Microchip," *Biotechnology Progress*, vol. 22, pp. 1416-1425, 2006.
- [6] L. Pollack, M. W. Tate, A. C. Finnefrock, C. Kalidas, S. Trotter, N. C. Darnton, L. Lurio, R. H. Austin, C. A. Batt, S. M. Gruner, and S. G. J. Mochrie, "Time resolved collapse of a folding protein observed with small angle X-ray scattering," *Physical Review Letters*, vol. 86, pp. 4962-4965, 2001.
- [7] P. A. George, W. Hui, F. Rana, B. G. Hawkins, A. E. Smith, and B. J. Kirby, "Microfluidic devices for terahertz spectroscopy of biomolecules," *Optics Express*, vol. 16, pp. 1577-1582, 2008.
- [8] K. Wallenfels and R. Weil, *Beta-galactosidase*, 3 ed. vol. 7. New York: Academic Press, 1972.
- [9] J. R. Beckwith, "Regulation of the lac operon. Recent studies on the regulation of lactose metabolism in *Escherichia coli* support the operon model," *Science FIELD Full Journal Title: Science (New York, N.Y.)*, vol. 156, pp. 597-604, 1967.
- [10] F. Jacob and J. Monod, "Genetic regulatory mechanisms in the synthesis of proteins," *Journal of Molecular Biology*, vol. 3, pp. 318-56, 1961.

- [11] G. R. Craven, E. Steers, Jr., and C. B. Anfinsen, "Purification, composition, and molecular weight of the b-galactosidase of *Escherichia coli* K12," *Journal of Biological Chemistry*, vol. 240, pp. 2468-77, 1965.
- [12] R. E. Huber, M. T. Gaunt, and K. L. Hurlburt, "Binding and reactivity at the \"glucose\" site of galactosyl-b-galactosidase (*Escherichia coli*)," *Archives of Biochemistry and Biophysics*, vol. 234, pp. 151-60, 1984.
- [13] R. E. Huber, G. Kurz, and K. Wallenfels, "A quantitation of the factors which affect the hydrolase and transgalactosylase activities of b-galactosidase (*E. coli*) on lactose," *Biochemistry*, vol. 15, pp. 1994-2001, 1976.
- [14] R. H. Jacobson, X. J. Zhang, R. F. DuBose, and B. W. Matthews, "Three-dimensional structure of b-galactosidase from *E. coli*," *Nature (London, United Kingdom)*, vol. 369, pp. 761-6, 1994.
- [15] U. Karlsson, S. Koorajian, I. Zabin, F. S. Sjostrand, and A. Miller, "High-resolution electron microscopy on highly purified b-galactosidase from *Escherichia coli*," *Journal of Ultrastructure Research*, vol. 10, pp. 457-69, 1964.
- [16] S. L. Marchesi, E. Steers, Jr., and S. Shifrin, "Purification and characterization of the multiple forms of b-galactosidase of *Escherichia coli*," *Biochimica et Biophysica Acta, Protein Structure*, vol. 181, pp. 20-34, 1969.
- [17] A. V. Fowler and I. Zabin, "Amino acid sequence of b-galactosidase. XI. Peptide ordering procedures and the complete sequence," *Journal of Biological Chemistry*, vol. 253, pp. 5521-5, 1978.
- [18] A. Kalnins, K. Otto, U. Ruether, and B. Mueller-Hill, "Sequence of the lacZ gene of *Escherichia coli*," *EMBO Journal*, vol. 2, pp. 593-7, 1983.
- [19] A. Nichtl, J. Buchner, R. Jaenicke, R. Rudolph, and T. Scheibel, "Folding and association of b-galactosidase," *Journal of Molecular Biology*, vol. 282, pp. 1083-1091, 1998.
- [20] S. Shifrin and E. Steers, Jr., "Effect of urea on subunit interaction of b-galactosidase from *Escherichia coli* K12," *Biochimica et Biophysica Acta, Protein Structure*, vol. 133, pp. 463-71, 1967.
- [21] A. Ullmann and J. Monod, "Effect of divalent cations and protein concentration upon renaturation of b-galactosidase from *Escherichia coli*," *Biochemical and Biophysical Research Communications*, vol. 35, pp. 35-42, 1969.

- [22] M. A. Unger, H.-P. Chou, T. Thorsen, A. Scherer, and S. R. Quake, "Monolithic microfabricated valves and pumps by multilayer soft lithography," *Science (Washington, D. C.)*, vol. 288, pp. 113-116, 2000.
- [23] D. C. Duffy, J. C. McDonald, O. J. A. Schueller, and G. M. Whitesides, "Rapid Prototyping of Microfluidic Systems in Poly(dimethylsiloxane)," *Analytical Chemistry*, vol. 70, pp. 4974-4984, 1998.
- [24] G. P. Nolan, S. Fiering, J. F. Nicolas, and L. A. Herzenberg, "Fluorescence-activated cell analysis and sorting of viable mammalian cells based on b-D-galactosidase activity after transduction of *Escherichia coli* lacZ," *Proceedings of the National Academy of Sciences of the United States of America*, vol. 85, pp. 2603-7, 1988.
- [25] B. Rotman, J. A. Zderic, and M. Edelstein, "Fluorogenic substrates for b-D-galactosidases and phosphatases derived from fluorescein (3,6-dihydroxyfluoran) and its mono-methyl ether," *Proceedings of the National Academy of Sciences of the United States of America*, vol. 50, pp. 1-6, 1963.
- [26] S. Lee, W. Jeong, and D. J. Beebe, "Microfluidic valve with cored glass microneedle for microinjection," *Lab on a Chip*, vol. 3, pp. 164-167, 2003.
- [27] T. Thorsen, S. J. Maerkl, and S. R. Quake, "Microfluidic Large-Scale Integration," *Science (Washington, DC, United States)*, vol. 298, pp. 580-584, 2002.
- [28] Y.-C. Wang, M. H. Choi, and J. Han, "Two-dimensional protein separation with advanced sample and buffer isolation Using microfluidic valves," *Analytical Chemistry*, vol. 76, pp. 4426-4431, 2004.
- [29] H.-P. Chou, M. A. Unger, and S. R. Quake, "A microfabricated rotary pump," *Biomedical Microdevices*, vol. 3, pp. 323-330, 2001.
- [30] Z. J. Huang, "Kinetic fluorescence measurement of fluorescein di-beta-D-galactoside hydrolysis by beta-galactosidase: intermediate channeling in stepwise catalysis by a free single enzyme," *Biochemistry FIELD Full Journal Title: Biochemistry*, vol. 30, pp. 8535-40, 1991.
- [31] D. L. Hevehan and E. De Bernardez Clark, "Oxidative renaturation of lysozyme at high concentrations," *Biotechnology and Bioengineering*, vol. 54, pp. 221-230, 1997.
- [32] G. Zettlmeissl, R. Rudolph, and R. Jaenicke, "Reconstitution of lactic dehydrogenase. Noncovalent aggregation vs. reactivation. 1. Physical properties and kinetics of aggregation," *Biochemistry*, vol. 18, pp. 5567-71, 1979.

- [33] L. Smeller, F. Meersman, and K. Heremans, "Refolding studies using pressure: The folding landscape of lysozyme in the pressure-temperature plane," *Biochimica et Biophysica Acta, Proteins and Proteomics*, vol. 1764, pp. 497-505, 2006.
- [34] A. Ayling and F. Beneyx, "Influence of the GroE molecular chaperone machine on the in vitro refolding of Escherichia coli b-galactosidase," *Protein Science*, vol. 5, pp. 478-87, 1996.

CHAPTER 3

INTEGRATED MICROFLUIDIC PRECONCENTRATOR AND IMMUNOBIOSENSOR

3.1 Abstract

We present a microfluidic biosensor that integrates membrane-based preconcentration with fluorescence detection. The concentration membrane was fabricated in polyacrylamide by *in-situ* photopolymerization technique at the junction of glass microchannels. Liposomes entrapping sulforhodamine B (SRB) dye molecules were used for signal amplification. The biotin-streptavidin binding system was a model system for evaluating device performance. Biotinylated liposomes were preconcentrated at the membrane by applying an electric field across the membrane. The electric field causes the liposomes to migrate towards the membrane where they are concentrated by a sieving effect. Two orders of magnitude concentration was achieved after applying the electric field for only 2 min. The concentrated bolus was then eluted towards the detection unit, where the biotinylated liposomes were captured by immobilized streptavidin. The integrated system with the preconcentration module shows a fourteen-fold improvement in signal as opposed to a system that does not include preconcentration.

3.2 Introduction

Microfluidic systems have become increasingly popular in biological and chemical analyses owing to the advantages of minimal reagent use, cost-effectiveness and automation [1-4]. An important application of microfluidic systems has been in the

field of biosensors for pathogen detection and clinical diagnostics [5-7]. However, the use of microfluidic devices for the total analysis of a whole sample has been limited due to the challenges associated with integration of the different processing steps like sample preparation, preconcentration, analysis and detection on the same device [8-12]. In this paper, we present an integrated microfluidic immunobiosensor that combines preconcentration and fluorescence detection steps to enable sensitive detection in dilute samples.

Preconcentration of sample prior to analysis is an important step in microfluidic systems as it enables detection of very small concentrations of analytes and also improves detection sensitivity and signal-to-noise ratios. A number of preconcentration techniques have been developed that can achieve high concentration factors in small time durations. Some examples include surface-binding techniques like solid-phase extraction [13-16] and electrokinetic manipulation techniques like isoelectric focusing [17-19], field-amplified sample stacking [20, 21], isotachopheresis [22-25] and dielectrophoresis [26, 27]. However, the limitations of these techniques are that they either involve buffer handling challenges or fabrication complexities making them difficult to integrate with lab-on-chip systems. Porous membrane-based preconcentration systems, on the other hand, do not involve complex buffer systems to concentrate samples. Khandurina *et al.* [28, 29] demonstrated the use of a porous silicate membrane while Wang *et al.* [30] used a nanofluidic filter for preconcentration. However, in the former case, the authors reported that the silicate membranes were hard to fabricate in a reproducible manner and the latter approach involves the fabrication of micro- and nanochannels in the same device. More recently, Kim *et al.* [31] have developed self-sealed nanoporous junctions inside PDMS microchannels for preconcentration. However, PDMS-based devices are less robust and are prone to surface adhesion and reusability issues.

We use an *in-situ* photopolymerized nanoporous membrane [32-34] in our integrated glass microfluidic device for the preconcentration step. Song *et al.* [32] have shown high concentration factors (four orders of magnitude local concentration) using these nanoporous membranes. The *in-situ* fabrication technique allows for easy integration with total analysis systems. Our membranes are fabricated in polyacrylamide as it is hydrophilic, biocompatible and shows minimal non-specific adhesion [34]. The pore-size of acrylamide gels can be easily adjusted by changing the percentage of monomer components [35, 36]. Moreover, unlike other membrane-based concentration methods, the response of this system is linear with the voltage-time product [32].

Figure 3.1 shows the integrated microfluidic biosensor with the insets showing the concentration membrane and the detection region. The membrane is nanoporous and is made using polyacrylamide at the intersection of the glass channels by an *in-situ* photopolymerization technique [32-34, 37-39]. We use liposomes, which can encapsulate a very large number of fluorescent dye molecules in their core for signal amplification in the biosensor. Fluorescence from the dye molecules is quenched when they are encapsulated at a high concentration within the liposome core. The analytes to be detected are tagged with liposomes and these complexes are injected into the inlet well of the device. An electric field is applied across the membrane, causing the liposome-analyte complexes to migrate towards the membrane. However, since the size of the pores in the membranes is much smaller than the size of these complexes, they are concentrated at the membrane by a sieving effect. The concentrated bolus is then eluted towards the detection region, where these complexes are captured using immobilized antibodies. The captured liposomes are then lysed by flowing a detergent and the released fluorophores result in a significant signal enhancement due to the elimination of self-quenching of the dye molecules.

In this paper, we present results showing improved detection sensitivity with the inclusion of the preconcentration system using proof-of-concept experiments performed with biotin-streptavidin binding.

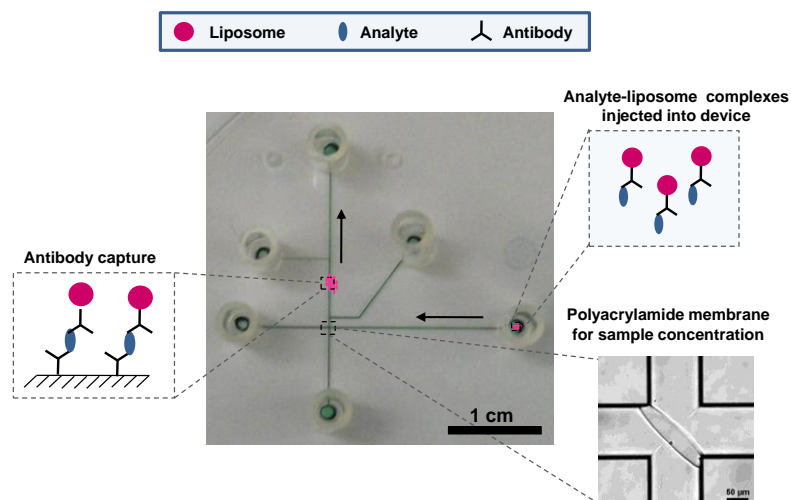


Figure 3.1: Image of the integrated glass microfluidic device with the channels filled with food dye to show contrast. The insets show a picture of the polyacrylamide membrane-based concentrator and schematics of antigen-antibody binding in the device.

3.3 *Experimental methods*

3.3.1 *Fabrication of microfluidic channels*

Schott D263 glass wafers (100 mm diameter, 0.55 mm thick; S I Howard Co., Worcester, MA) were used for etching microfluidic channels. Device geometry was defined using L-Edit CAD software (Tanner Research) and a photomask was created using GCA/Mann 3600F Optical Pattern Generator. A 225nm thick layer of amorphous silicon deposited on the glass wafers by PECVD was used as the hard mask for etching. The wafers were then coated with a 3μm thick layer of Shipley 1818

positive photoresist and soft-baked at 115°C for 1 min. The mask pattern was transferred to the photoresist using an EV 620 contact aligner and the wafers were developed using a 300MIF resist developer. The exposed silicon was etched using an Oxford 80 (#1) reactive ion etching (RIE) system and the photoresist was stripped using a mixture of acetone and isopropanol. The exposed glass was etched using a 16% HF solution (Shape Products Company, Oakland, CA). The glass wafers were exposed to HF for 14 min, resulting in channel depths of 20 μm (etch rate of D263 glass in 16% HF is about 1.4 $\mu\text{m}/\text{min}$ when left unagitated). Finally, the remaining silicon on the wafers was removed by reactive ion etching using the Oxford 80 (#1) system. In the final device, the wide channel width was 120 μm and the narrow channel width was 50 μm . The depths of the channels in both cases were 20 μm . Connection holes were made in the wafers by sandblasting.

3.3.2 Wafer bonding

The glass microchannels were sealed by a plain borofloat glass wafer (100 mm diameter, 500 μm thick; Mark Optics, Santa Ana, CA) using a low temperature glass bonding technique [28, 29, 40, 41]. The etched and the plain glass wafers were cleaned by sonicating in acetone for about 5 min. The wafers were then hydrolyzed in RCA cleaning solution (prepared by mixing 5N ammonium hydroxide, 30% w/w hydrogen peroxide and deionized water in 3:2:9 ratio by volume) for 20 min at 70-80 °C, rinsed in deionized water and dried under nitrogen. This was followed by plasma cleaning to activate the surfaces of both the wafers prior to bonding. A thin layer of potassium silicate (KASIL 2130, The PQ Corp., Valley Forge, PA) was coated on the plain glass wafer by spinning a diluted solution (1:10 by weight in deionized water) at 2000 rpm for 8s. As the spin-coated wafer was then brought into contact with the

etched glass wafer, the bonding region spread instantaneously across the entire area of the wafers. The bonded wafers were then placed in a hot press at 90 °C for an hour to reinforce the bonding.

3.3.3 Membrane fabrication and surface treatment

The channels of the bonded devices were treated with 1M NaOH for 20 min to remove the potassium silicate layer in the microchannels. The wafers were then rinsed with DI water and dried in nitrogen. Prior to membrane fabrication, the glass channels were coated with an acrylate-terminated self-assembling monolayer to enable covalent attachment of the polyacrylamide membrane to the channel walls[42-44]. For this, the channels were prepared by exposing to 1M HCl for 30min, rinsing in DI water and then exposing to 1M NaOH for 30 min. The channels were thoroughly rinsed with DI water and then exposed to a freshly mixed coating solution containing 2:3:5 mixture (by volume) of 3-(trimethoxysilyl)propyl acrylate, glacial acetic acid and deionized water for exactly 30 min. The channels were finally rinsed in 1-propanol and DI water and dried with vacuum.

The polyacrylamide membrane was fabricated at the intersection of the glass microchannels by a photopolymerization technique [32-34, 37-39]. For this, a 355 nm laser beam was shaped using a train of lenses and mirrors into a long narrow beam to match the dimensions of the channel junction. The optical train also helps to direct the beam through a microscope to enable visualization of the polymerization process. The channels were filled with a freshly prepared and degassed solution of 22% (15.7:1) acrylamide/bisacrylamide containing 0.2% (w/v) VA-086 photoinitiator [34]. All the reservoirs were capped with tape to prevent evaporation, and the solution was allowed to equilibrate for 20 min to eliminate pressure-driven flow. The membrane was then

fabricated by directing the shaped laser beam towards the junction and exposing for approximately 15s. The unpolymerized acrylamide solution was purged from the channels and the channels were rinsed thoroughly with DI water.

Finally, the channels were coated with linear polyacrylamide to suppress the electroosmotic flow [42-44]. The channels were filled with a degassed solution of 50 mg/ml acrylamide in deionized water containing 250 ppm hydroquinone and 2 mg/ml V-50 photoinitiator and exposed to UV light in a UV oven for 30 min. The unpolymerized solution was rinsed out of the channels and the channels were cleaned with DI water.

3.3.4 Liposome and magnetic bead preparation

Liposomes were prepared by a modified version [45] of the reversed-phase evaporation technique described by Siebert et al [46]. All lipids used were obtained from Avanti Polar Lipids (Alabaster, AL). Fluorescent liposomes encapsulate 150mM sulforhodamine B (SRB) dye in 0.02M HEPES, pH 7.5 in the core and also contain 0.33mol% dipalmitoyl phosphoethanolamine (DPPE)-rhodamine in the bilayer. Biotinylated lipids were used in the preparation of the liposomes in order to add functionality to the outer surface of the bilayer. The remainder of the bilayer consists of 35mol% dipalmitoyl phosphatidylcholine (DPPC), 15mol% dipalmitoyl phosphatidylglycerol (DPPG), 42mol% cholesterol, and 6mol% N-(glutaryl)-1,2-dipalmitoyl-*sn*-glycero-3-phosphoethanolamine. After formation of the vesicles, extrusions through 1 μ m and 0.4 μ m filters was performed to assure unilamellar liposomes with a uniform size distribution. Removal of unencapsulated SRB was facilitated by application of the liposome preparation to a Sephadex G-50 column equilibrated with 0.01 M HEPES, pH 7.5, containing 0.2 M NaCl, 0.2 M sucrose, and

0.01% sodium azide (NaN_3). Fractions containing liposomes were collected and dialyzed against 0.01 M HEPES, 0.2 M NaCl, 0.2 M sucrose, 0.01% NaN_3 pH 7.5 (1XHSS) in the dark overnight.

To capture these biotinylated liposomes in the microfluidic device, commercially available streptavidin-conjugated superparamagnetic beads (Dynabeads MyOne Streptavidin, 1 μm in diameter; Invitrogen, Carlsbad, CA) were used. Prior to use, the stock was vortexed to homogenize the suspension and the necessary volume was removed. In order to remove preservatives and introduce the working buffer, the beads were then washed twice with an equal volume of 1XHSS by applying the tube to a magnet rack, removing the supernatant, and resuspending.

3.3.5 Sample loading, concentration and detection

Prior to performing concentration and detection experiments, the channels of the device were primed with 1X HSS buffer. A permanent magnet was positioned on the top surface of the device upstream of the detection region using adhesive putty. 1 μl of Dynabeads MyOne streptavidin-conjugated superparamagnetic beads prepared in 1X HSS buffer was injected towards the magnet through the port 5 (Figure 3.2) using a syringe pump at a flow rate of 1 $\mu\text{l}/\text{min}$. For the electrokinetic concentration experiments, a solution of 10,000x diluted fluorescent liposomes (biotinylated with SRB dye in the core) in HSS buffer was used. For the direct injection experiments, the liposome solution was further diluted by a factor of 10 in HSS buffer (due to lowest achievable flow rate limitations with our existing equipment) so that the same number of liposomes is flowed through the device for performance comparison.

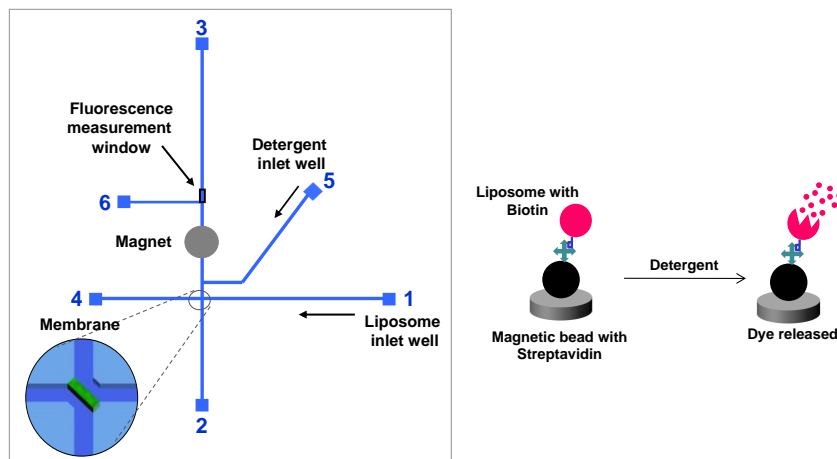


Figure 3.2: Schematic of device used for the biotin-streptavidin experiments in fluorescence detection mode. Biotinylated liposomes are captured by streptavidin-conjugated magnetic beads localized at the magnet. The fluorescence from the lysed liposomes is imaged downstream from the magnet in the region marked as the fluorescence measurement window.

For the direct injection experiments, the biotinylated liposome solution in HSS buffer was injected towards the magnet with a syringe pump at a flow rate of 10 $\mu\text{l/h}$ for 90s through inlet port 1 (Figure 3.2). After liposome injection, wash buffer was injected at a flow rate of 20 $\mu\text{l/h}$ to wash off any unbound liposomes in the device through port 5. A detergent solution of 60mM octyl- β -D-glucopyranoside (OG) was then flowed through the same port 5 towards the bead bed at a flow rate of 40 $\mu\text{l/h}$ and the emitted fluorescence from the lysis of the liposomes was recorded downstream of the bead bed.

For the electrokinetic concentration experiment, all the wells were filled with 60 μl of plain HSS buffer except the inlet well which was filled with the liposome-HSS solution. The pressure driven flow in the system was eliminated by adjusting the heights of the solutions in the wells. The liposomes were then electrophoretically concentrated at the membrane by applying a voltage difference of 150V across the membrane. After concentrating for a duration of 90s, the concentrated bolus of

liposomes was eluted towards the bead bed by applying a voltage of 150V to the outlet port 3 downstream of the magnet. The wash buffer and OG solutions were injected at the same flow rates as in the above case through port 5 and the fluorescence signal from the lysed liposomes was recorded downstream of the magnet.

For each experiment, the background was calculated as the average of the total fluorescence intensity values estimated in the region of interest during the first 60 frames of the detergent injection videos.

After each run, the device was thoroughly rinsed with deionized water multiple times followed by a final rinse which involves flowing deionized water at a rate of 2 $\mu\text{l}/\text{min}$ with a syringe pump for 15 min.

3.4 Results

3.4.1 *Electrophoretic concentration of fluorescent liposomes*

Concentration and elution experiments were performed using fluorescent liposomes to estimate the concentration factors for the membrane-based preconcentration system. Figure 3.3 shows snapshots of the channel junction during the concentration and elution steps achieved by switching electric fields between the vertical and horizontal channels. Figure 3.4 shows the concentration factor plotted as a function of time for which the high voltage is applied across ports 1 and 4 (Figure 3.3(a)). It can be seen from Figure 3.4 that after a concentration time of 160s, the estimated concentration

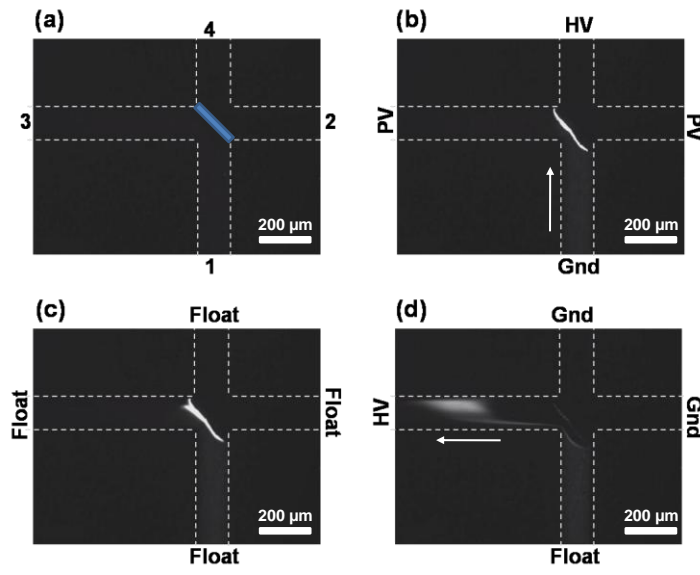


Figure 3.3: Image sequence showing liposome concentration and elution. Microchannel edges have been drawn for clarity. The membrane has also been highlighted in blue in Figure 3.3(a). HV denotes high voltage (100V), PV pinch voltage (40V), Gnd ground. (a) Before loading (b) Sample concentration (c) After concentration (d) Sample elution. Pinch voltage is applied to minimize the diffusion of the sample away from the membrane.

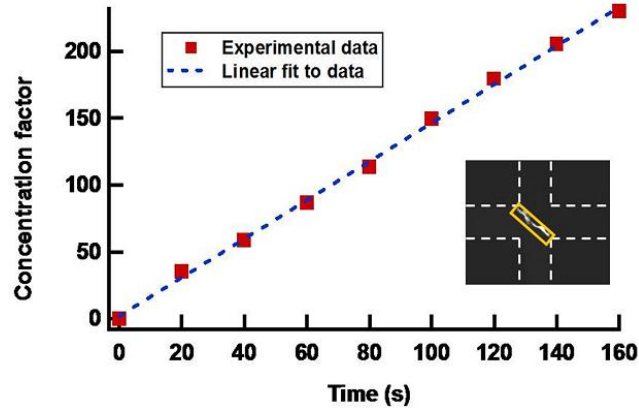


Figure 3.4: Concentration factors during liposome concentration as a function of time. The intensities were averaged over a measurement window (23 x 180 pixels) shown as a box in the inset. The concentration factors are consistent with analytical values estimated using a liposome zeta potential of -19mV.

factor was around 230. Analytical calculations resulted in concentration factors of around 350 for 160s of applying high voltage which is on the same order of magnitude as the experimental value. For these calculations, the zeta potential of the liposomes estimated from Zetasizer measurements was -28.8 ± 2.9 mV (resulting in a mean electrophoretic velocity of $103.1 \mu\text{m/s}$), while the inferred zeta potential from the experiments was -19 mV. The trend in Figure 3.4 is linear as expected as the liposomes migrate with a constant electrophoretic velocity.

3.4.2 Integrated concentration and detection experiments

Concentration and detection experiments were performed with the biotin-streptavidin binding system in the integrated microfluidic device. For these experiments, biotinylated fluorescent liposomes (with SRB dye in the core and bilayer) were used as the analytes to be detected. Streptavidin coated magnetic beads immobilized in the channels using a permanent magnet served as the capture region. The liposomes were electrophoretically concentrated at the membrane by applying a high voltage across the membrane. The concentrated bolus of liposomes was eluted by switching the electric field towards the bead bed where the liposomes are captured. Figure 3.5 shows an image of the bead bed with the captured fluorescent liposomes. The unbound liposomes were washed away by flowing 1X HSS as wash buffer over the bead bed. The OG solution was then injected into the channels, resulting in the lysis of the bound liposomes. The released fluorescence from the liposomes was captured downstream in the region indicated as the fluorescence measurement window in Figure 3.2. Snapshots from the fluorescence burst during OG injection in the region of interest are shown in Figure 3.6.

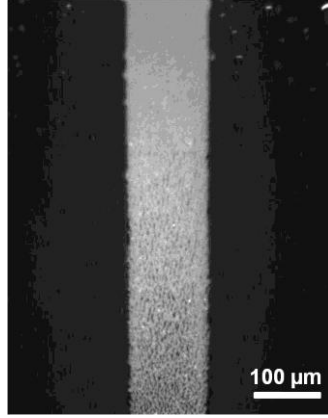


Figure 3.5: Fluorescent liposomes captured at the bead bed immobilized using a permanent magnet.

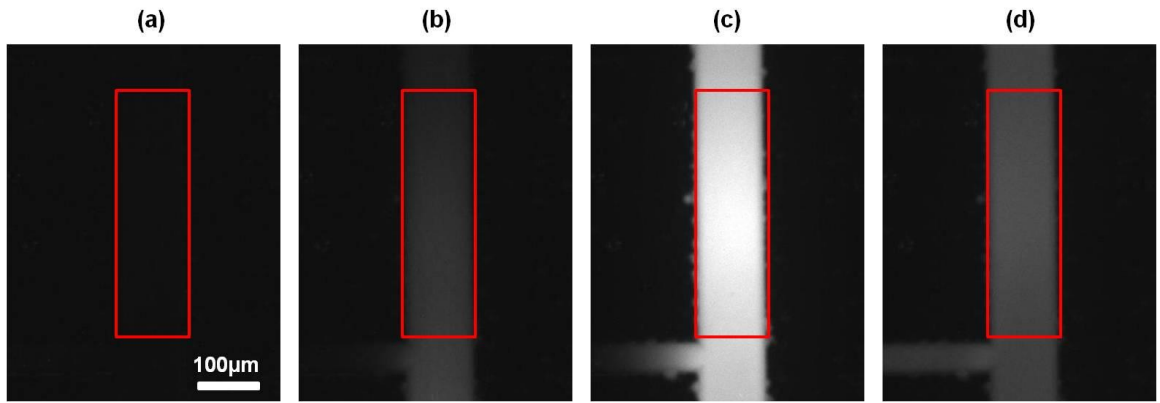


Figure 3.6: Snapshots of the fluorescence measurement window (shown as a red box) during OG injection. (a): Background image before the start of injection. (b), (c), (d): Snapshots during fluorescence burst from the lysed liposomes during OG injection.

3.4.3 Comparison of device performance with and without concentration

In order to evaluate the effect of the preconcentration step on the performance of the system, direct injection experiments were performed where the liposomes were injected towards the bead bed using a syringe pump bypassing the concentration step.

The number of liposomes in the device was maintained the same for both sets of experiments – with and without the preconcentration step.

The total fluorescence intensity in the measurement window during OG injection was estimated from the captured videos of fluorescence burst and plotted as a function of time. These intensity profiles are shown in Figure 3.7. This figure shows data from both the electrokinetic concentration (shown in red) and direct injection (shown in blue) experiments. The area under these curves gives the integrated fluorescence intensities for each of these experiments. These integrated intensities for the electrokinetic concentration and direct injection cases are compared in Figure 3.8. This figure shows that the inclusion of the preconcentration step increases the signal by a factor of 14. The increased signal is a result of a concentrated bolus of liposomes flowing over the bead bed resulting in better capture efficiencies than in the case where a dilute solution of the same number of liposomes is flowed.

3.5 Discussion

The detection sensitivity of the biosensor depends on the binding kinetics between the low concentration of an analyte and the surface immobilized biorecognition element. This process is usually diffusion-limited [47-49], and an increase in the local analyte concentration in the capture region greatly improves the binding kinetics. Singh and coworkers [10, 34] have used similar membrane-based preconcentrators in conjunction with microchip SDS-PAGE and electrophoretic immunoassays to show improved separation resolution and detection limits. Wang *et al.* [50] have shown 500-fold improvement in sensitivity (from 50 pM to sub 100fM) and improved dynamic range of immunoassay detection using nanofluidic filter based electrokinetic

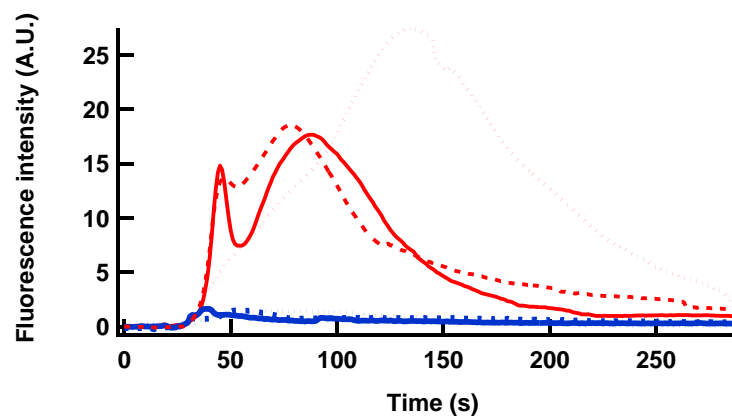


Figure 3.7: Fluorescence intensity profiles from the bead bed during OG injection for the two experiments including the preconcentration step (shown in red lines) and excluding it (shown in blue lines).

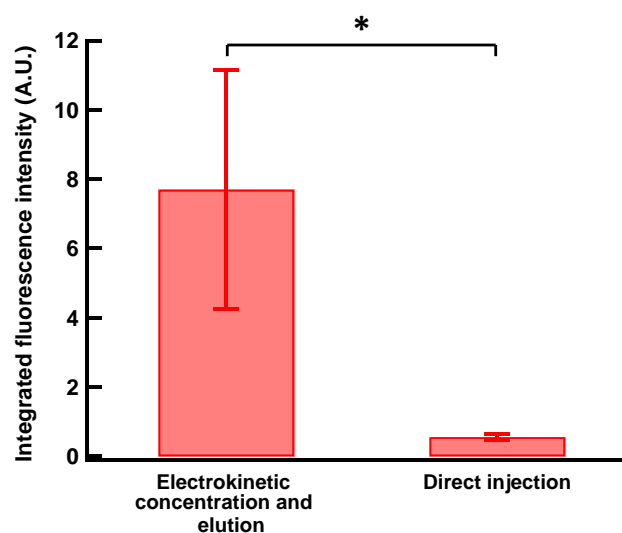


Figure 3.8: Comparison of the effect of preconcentration on the integrated fluorescence intensities from the bead bed during OG injection. The data is reported as mean \pm SD with $n=3$. * indicates $p<0.05$.

preconcentrator. However, this device has fabrication complexities as it involves etching of both micro- and nanochannels in the same device. Also, the improvement in sensitivity has been reported for molecular analytes like proteins and does not include any post-binding amplification steps.

Our design and fabrication techniques are compatible for integrating electrochemical detection into the device. The device can be operated in electrochemical detection mode by patterning gold interdigitated electrodes downstream from the membrane and using electrochemical liposomes instead of fluorescent ones [51]. The low temperature bonding technique is suitable for bonding etched glass wafers with gold-patterned wafers as it does not lead to delamination of the gold electrodes as seen in the conventional high temperature bonding techniques. Also, the core of the liposomes can be filled with electrochemical species such as potassium ferri/ferro hexacyanide molecules instead of fluorophores for detection. This straightforward extension to an electrochemical system is advantageous as electrochemical detection methods offer several benefits over popularly used optical detection techniques. These include low capital cost for equipment, portability, low power requirement and lack of photobleaching issues [52, 53].

3.6 Conclusion

In conclusion, we have presented an integrated microfluidic biosensor that integrates on-chip concentration with liposome-based signal amplification on the same device. We have achieved two orders of magnitude concentration with the membrane-based system within 160s of applying high voltage across the membrane. The electric field can be switched to elute the concentrated sample bolus towards the detection region

where it is captured efficiently at the immobilized bead bed. The inclusion of the preconcentration step results in a fourteen-fold improvement in the signal as opposed to a system without the preconcentration step, when the same number of liposomes is introduced in both cases. The functionality of the membrane can be extended to a filtering device for removing small interfering particles that competitively bind to the target probes, further increasing the signal-to-noise ratio.

3.7 Acknowledgements

This work was supported by the United States Environmental Protection Agency and was performed in part at the Cornell Nanofabrication Facility. The authors would like to thank K. A. Edwards for providing fluorescent liposomes used in the early concentration experiments.

BIBLIOGRAPHY

- [1] A. Arora, G. Simone, G. B. Salieb-Beugelaar, J. T. Kim, and A. Manz, "Latest Developments in Micro Total Analysis Systems," *Anal. Chem. (Washington, DC, U. S.)*, vol. 82, pp. 4830-4847, 2010.
- [2] P.-A. Auroux, D. Iossifidis, D. R. Reyes, and A. Manz, "Micro Total Analysis Systems. 2. Analytical Standard Operations and Applications," *Anal. Chem.*, vol. 74, pp. 2637-2652, 2002.
- [3] K.-i. Ohno, K. Tachikawa, and A. Manz, "Microfluidics: applications for analytical purposes in chemistry and biochemistry," *Electrophoresis*, vol. 29, pp. 4443-4453, 2008.
- [4] D. R. Reyes, D. Iossifidis, P.-A. Auroux, and A. Manz, "Micro Total Analysis Systems. 1. Introduction, Theory, and Technology," *Anal. Chem.*, vol. 74, pp. 2623-2636, 2002.
- [5] J. Mairhofer, K. Roppert, and P. Ertl, "Microfluidic systems for pathogen sensing: a review," *Sensors*, vol. 9, pp. 4804-4823, 2009.
- [6] P. Liu and R. A. Mathies, "Integrated microfluidic systems for high-performance genetic analysis," *Trends Biotechnol.*, vol. 27, pp. 572-581, 2009.
- [7] L. Chen, A. Manz, and P. J. R. Day, "Total nucleic acid analysis integrated on microfluidic devices," *Lab Chip*, vol. 7, pp. 1413-1423, 2007.
- [8] N. Beyor, L. Yi, T. S. Seo, and R. A. Mathies, "Integrated Capture, Concentration, Polymerase Chain Reaction, and Capillary Electrophoretic Analysis of Pathogens on a Chip," *Anal. Chem. (Washington, DC, U. S.)*, vol. 81, pp. 3523-3528, 2009.
- [9] R. Sista, Z. Hua, P. Thwar, A. Sudarsan, V. Srinivasan, A. Eckhardt, M. Pollack, and V. Pamula, "Development of a digital microfluidic platform for point of care testing," *Lab Chip*, vol. 8, pp. 2091-2104, 2008.
- [10] A. E. Herr, A. V. Hatch, D. J. Throckmorton, H. M. Tran, J. S. Brennan, W. V. Giannobile, and A. K. Singh, "Microfluidic immunoassays as rapid saliva-based clinical diagnostics," *Proc. Natl. Acad. Sci. U. S. A.*, vol. 104, pp. 5268-5273, 2007.
- [11] C. J. Easley, J. M. Karlinsey, J. M. Bienvenue, L. A. Legendre, M. G. Roper, S. H. Feldman, M. A. Hughes, E. L. Hewlett, T. J. Merkel, J. P. Ferrance, and J. P. Landers, "A fully integrated microfluidic genetic analysis system with

sample-in-answer-out capability," *Proc. Natl. Acad. Sci. U. S. A.*, vol. 103, pp. 19272-19277, 2006.

- [12] E. T. Lagally, J. R. Scherer, R. G. Blazej, N. M. Toriello, B. A. Diep, M. Ramchandani, G. F. Sensabaugh, L. W. Riley, and R. A. Mathies, "Integrated Portable Genetic Analysis Microsystem for Pathogen/Infectious Disease Detection," *Anal. Chem.*, vol. 76, pp. 3162-3170, 2004.
- [13] J. D. Ramsey and G. E. Collins, "Integrated microfluidic device for solid-phase extraction coupled to micellar electrokinetic chromatography separation," *Anal. Chem.*, vol. 77, pp. 6664-6670, 2005.
- [14] B. S. Broyles, S. C. Jacobson, and J. M. Ramsey, "Sample filtration, concentration, and separation integrated on microfluidic devices," *Anal. Chem.*, vol. 75, pp. 2761-2767, 2003.
- [15] A. B. Jemere, R. D. Oleschuk, F. Ouchen, F. Fajuyigbe, and D. J. Harrison, "An integrated solid-phase extraction system for sub-picomolar detection," *Electrophoresis*, vol. 23, pp. 3537-3544, 2002.
- [16] C. Yu, M. H. Davey, F. Svec, and J. M. J. Frechet, "Monolithic porous polymer for on-chip solid-phase extraction and preconcentration prepared by photoinitiated in situ polymerization within a microfluidic device," *Anal. Chem.*, vol. 73, pp. 5088-5096, 2001.
- [17] Y. Li, D. L. DeVoe, and C. S. Lee, "Dynamic analyte introduction and focusing in plastic microfluidic devices for proteomic analysis," *Electrophoresis*, vol. 24, pp. 193-199, 2003.
- [18] W. Tan, Z. H. Fan, C. X. Qiu, A. J. Ricco, and I. Gibbons, "Miniaturized capillary isoelectric focusing in plastic microfluidic devices," *Electrophoresis*, vol. 23, pp. 3638-3645, 2002.
- [19] C. R. Cabrera and P. Yager, "Continuous concentration of bacteria in a microfluidic flow cell using electrokinetic techniques," *Electrophoresis*, vol. 22, pp. 355-362, 2001.
- [20] B. Jung, R. Bharadwaj, and J. G. Santiago, "Thousandfold signal increase using field-amplified sample stacking for on-chip electrophoresis," *Electrophoresis*, vol. 24, pp. 3476-3483, 2003.
- [21] J. Lichtenberg, E. Verpoorte, and N. F. de Rooij, "Sample preconcentration by field amplification stacking for microchip-based capillary electrophoresis," *Electrophoresis*, vol. 22, pp. 258-271, 2001.

- [22] B. Jung, R. Bharadwaj, and J. G. Santiago, "On-Chip Millionfold Sample Stacking Using Transient Isotachopheresis," *Anal. Chem.*, vol. 78, pp. 2319-2327, 2006.
- [23] W. N. Vreeland, S. J. Williams, A. E. Barron, and A. P. Sassi, "Tandem isotachopheresis-zone electrophoresis via base-mediated destacking for increased detection sensitivity in microfluidic systems," *Anal. Chem.*, vol. 75, pp. 3059-3065, 2003.
- [24] A. Wainright, S. J. Williams, G. Ciambone, Q. Xue, J. Wei, and D. Harris, "Sample pre-concentration by isotachopheresis in microfluidic devices," *J. Chromatogr., A*, vol. 979, pp. 69-80, 2002.
- [25] J. Wang, Y. Zhang, M. R. Mohamadi, N. Kaji, M. Tokeshi, and Y. Baba, "Exceeding 20 000-fold concentration of protein by the on-line isotachopheresis concentration in poly(methyl methacrylate) microchip," *Electrophoresis*, vol. 30, pp. 3250-3256, 2009.
- [26] B. H. Lapizco-Encinas, R. V. Davalos, B. A. Simmons, E. B. Cummings, and Y. Fintschenko, "An insulator-based (electrodeless) dielectrophoretic concentrator for microbes in water," *J. Microbiol. Methods*, vol. 62, pp. 317-326, 2005.
- [27] H. Moncada-Hernandez and B. H. Lapizco-Encinas, "Simultaneous concentration and separation of microorganisms: insulator-based dielectrophoretic approach," *Anal. Bioanal. Chem.*, vol. 396, pp. 1805-1816, 2010.
- [28] J. Khandurina, S. C. Jacobson, L. C. Waters, R. S. Foote, and J. M. Ramsey, "Microfabricated Porous Membrane Structure for Sample Concentration and Electrophoretic Analysis," *Anal. Chem.*, vol. 71, pp. 1815-1819, 1999.
- [29] R. S. Foote, J. Khandurina, S. C. Jacobson, and J. M. Ramsey, "Preconcentration of proteins on microfluidic devices using porous silica membranes," *Anal. Chem.*, vol. 77, pp. 57-63, 2005.
- [30] Y.-C. Wang, A. L. Stevens, and J. Han, "Million-fold Preconcentration of Proteins and Peptides by Nanofluidic Filter," *Anal. Chem.*, vol. 77, pp. 4293-4299, 2005.
- [31] S. J. Kim and J. Han, "Self-sealed vertical polymeric nanoporous-junctions for high-throughput nanofluidic applications. [Erratum to document cited in CA148:373127]," *Anal. Chem. (Washington, DC, U. S.)*, vol. 80, p. 7179, 2008.

- [32] S. Song, A. K. Singh, and B. J. Kirby, "Electrophoretic Concentration of Proteins at Laser-Patterned Nanoporous Membranes in Microchips," *Anal. Chem.*, vol. 76, pp. 4589-4592, 2004.
- [33] S. Song, A. K. Singh, T. J. Shepodd, and B. J. Kirby, "Microchip dialysis of proteins using in situ photopatterned nanoporous polymer membranes," *Anal. Chem.*, vol. 76, pp. 2367-2373, 2004.
- [34] A. V. Hatch, A. E. Herr, D. J. Throckmorton, J. S. Brennan, and A. K. Singh, "Integrated Preconcentration SDS-PAGE of Proteins in Microchips Using Photopatterned Cross-Linked Polyacrylamide Gels," *Anal. Chem.*, vol. 78, pp. 4976-4984, 2006.
- [35] D. L. Holmes and N. C. Stellwagen, "Estimation of polyacrylamide gel pore size from Ferguson plots of normal and anomalously migrating DNA fragments. I. Gels containing 3% N,N'-methylenebisacrylamide," *Electrophoresis (Weinheim, Fed. Repub. Ger.)*, vol. 12, pp. 253-63, 1991.
- [36] D. L. Holmes and N. C. Stellwagen, "Estimation of polyacrylamide gel pore size from Ferguson plots of linear DNA fragments. II. Comparison of gels with different crosslinker concentrations, added agarose and added linear polyacrylamide," *Electrophoresis (Weinheim, Fed. Repub. Ger.)*, vol. 12, pp. 612-19, 1991.
- [37] J. Han and A. K. Singh, "Rapid protein separations in ultra-short microchannels: microchip sodium dodecyl sulfate-polyacrylamide gel electrophoresis and isoelectric focusing," *J. Chromatogr., A*, vol. 1049, pp. 205-209, 2004.
- [38] A. E. Herr and A. K. Singh, "Photopolymerized Cross-Linked Polyacrylamide Gels for On-Chip Protein Sizing," *Anal. Chem.*, vol. 76, pp. 4727-4733, 2004.
- [39] D. J. Throckmorton, T. J. Shepodd, and A. K. Singh, "Electrochromatography in microchips: reversed-phase separation of peptides and amino acids using photopatterned rigid polymer monoliths," *Anal. Chem.*, vol. 74, pp. 784-789, 2002.
- [40] H. Y. Wang, R. S. Foote, S. C. Jacobson, J. H. Schneibel, and J. M. Ramsey, "Low temperature bonding for microfabrication of chemical analysis devices," *Sens. Actuators, B*, vol. B45, pp. 199-207, 1997.
- [41] J. Khandurina, T. E. McKnight, S. C. Jacobson, L. C. Waters, R. S. Foote, and J. M. Ramsey, "Integrated system for rapid PCR-based DNA analysis in microfluidic devices," *Anal. Chem.*, vol. 72, pp. 2995-3000, 2000.

- [42] B. J. Kirby, A. R. Wheeler, R. N. Zare, J. A. Fruetel, and T. J. Shepodd, "Programmable modification of cell adhesion and zeta potential in silica microchips," *Lab on a Chip*, vol. 3, pp. 5-10, 2003.
- [43] S. Hjerten, "Free zone electrophoresis," *Chromatogr Rev*, vol. 9, pp. 122-219, 1967.
- [44] S. Hjerten, "High-performance electrophoresis. Elimination of electroendosmosis and solute adsorption," *J. Chromatogr.*, vol. 347, pp. 191-8, 1985.
- [45] K. Edwards, K. Curtis, J. Sailor, and A. Baeumner, "Universal liposomes: preparation and usage for the detection of mRNA," *Analytical and Bioanalytical Chemistry*, vol. 391, pp. 1689-1702, 2008.
- [46] S. T. A. Siebert, S. G. Reeves, and R. A. Durst, "Liposome immunomigration field assay device for Alachlor determination," *Anal. Chim. Acta*, vol. 282, pp. 297-305, 1993.
- [47] A. Munir, J. Wang, Z. Li, and H. S. Zhou, "Numerical analysis of a magnetic nanoparticle-enhanced microfluidic surface-based bioassay," *Microfluid. Nanofluid.*, vol. 8, pp. 641-652, 2010.
- [48] A. Sadana and D. Sii, "Binding kinetics of antigen by immobilized antibody: influence of reaction order and external diffusional limitations," *Biosens. Bioelectron.*, vol. 7, pp. 559-68, 1992.
- [49] W. Kusnezow, Y. V. Syagailo, S. Rueffer, K. Klenin, W. Sebald, J. D. Hoheisel, C. Gauer, and I. Goychuk, "Kinetics of antigen binding to antibody microspots: strong limitation by mass transport to the surface," *Proteomics*, vol. 6, pp. 794-803, 2006.
- [50] Y.-C. Wang and J. Han, "Pre-binding dynamic range and sensitivity enhancement for immuno-sensors using nanofluidic preconcentrator," *Lab Chip*, vol. 8, pp. 392-394, 2008.
- [51] V. N. Goral, N. V. Zaytseva, and A. J. Baeumner, "Electrochemical microfluidic biosensor for the detection of nucleic acid sequences," *Lab Chip*, vol. 6, pp. 414-421, 2006.
- [52] S. Kwakye, V. N. Goral, and A. J. Baeumner, "Electrochemical microfluidic biosensor for nucleic acid detection with integrated minipotentiostat," *Biosens. Bioelectron.*, vol. 21, pp. 2217-2223, 2006.
- [53] S. Kwakye and A. Baeumner, "An embedded system for portable electrochemical detection," *Sens. Actuators, B*, vol. B123, pp. 336-343, 2007.

CHAPTER 4

**MICRO-TOTAL ANALYSIS SYSTEM FOR VIRUS DETECTION –
MICROFLUIDIC PRECONCENTRATION COUPLED TO
LIPOSOME-BASED DETECTION**

4.1 Abstract

In this work, an integrated microfluidic biosensor is presented, that combines sample preconcentration and liposome-based signal amplification for the detection of enteric viruses in environmental water samples. This microfluidic approach has the potential to overcome the challenges of long culture times for cell-culture methods and the need to extensively process water samples to eliminate inhibitors for PCR-based methods. In-situ fabricated nanoporous membranes in glass microchannels were used in conjunction with electric fields to achieve preconcentration of virus-liposome complexes. The concentrated complexes were eluted to a detection region downstream and the captured liposomes were lysed to release fluorescent dye molecules that were quantified using image processing. Detection experiments were performed on Feline Calicivirus (FCV), which was chosen as the model organism for human enteric virus. The limit of detection of FCV estimated with the integrated device was an order of magnitude lower than that obtained using a device which does not include preconcentration. This improved detection sensitivity indicates that the integrated device has the potential to serve as an early screening system for viruses in environmental water samples.

4.2 Introduction

Enteric viruses are any one of over 100 species that infect humans or animals via the fecal-oral route and primarily infect and replicate in the gastrointestinal tract. Though these viruses are commonly associated with gastroenteritis they can cause a range of diseases including respiratory infections, hepatitis, conjunctivitis and meningitis [1]. They have even been linked to chronic diseases like insulin-dependent diabetes [2].

Once infected, humans or host animals shed virus particles in feces. Enteric viruses are then introduced into water systems mostly through leaking sewage and septic systems, urban and agricultural runoff, and directly from untreated or under-treated wastewater. Outbreaks have been linked to not only contaminated drinking water, but also to contaminated recreational and irrigation water as well as shellfish harvested from contaminated waters [3]. These pathogenic viruses are highly resistant to changes in pH and temperature as well as to common methods of wastewater treatment. It has been shown that these viruses can remain infective up to 130 days in seawater, 120 days in freshwater and sewage, and 100 days in soil [1]. Depending on the source of contamination and water supply in question, virus particles can present in low concentrations complicating both detection and sterilization methods.

Current detection methods for enteric viruses can be divided into two main categories, cell culture assays and molecular methods. The cell culture technique was the most popular method for detection of enteric viruses prior to the development of the Polymerase Chain Reaction (PCR) and remains the method of choice to isolate and determine infectivity of viruses. The cell culture technique requires the inoculation of a cell line, chosen based on the virus of interest, and incubating for days to weeks as it is evaluated for the cytopathogenic effects of a viral infection [4]. This long incubation time is an obvious drawback of the cell culture assay though is not the only; some

viruses do not grow on established culture lines, grow too slowly, or just do not show any visible cytopathogenic effects.

The molecular methods most commonly used for the detection of enteric viruses are variations of conventional PCR [5] or reverse transcriptase-PCR (RT-PCR) [6], including real-time PCR [7] and multiplex PCR [8], as well as Nucleic Acid Sequence-Based Amplification (NASBA) [9]. These methods allow for the rapid, sensitive, and specific detection of enteric viruses of interest. The primary drawback to these molecular methods is the inability to limit detection to only infective viruses. However, this can be remedied by the use of integrated cell culture RT-PCR. This method involves inoculating a cell line with the sample and incubating for a short time, usually far before cytopathogenic effects are evident. Nucleic acids can then be extracted from the culture and processed through RT-PCR, testing for viral mRNA that would be produced only if the sample contained infective viruses. This process can, however, decrease the efficiency of detection [10].

As some enteric viruses are not cultivable and molecular techniques sacrifice efficiency of detection for an ability to identify infective viruses, many countries, including the United States, rely on indicators of fecal contamination - enterococci, coliform bacteria - rather than direct testing. Reliance on these indicators is flawed as viruses are more resistant to disinfection processes and natural environmental conditions [11, 12].

Feline Calicivirus (FCV) is a member of the *caliciviridae* family that causes respiratory and potentially severe systemic disease in cats. As it is non-pathogenic to humans and a member of the same family, FCV is used as a model for human pathogenic noroviruses [13]. Enzyme-Linked Immunosorbent Assays (ELISAs) for the detection of FCV have been previously described using two antibodies [14] and an antibody and a transmembrane glycoprotein [15]. Detection limits were not reported

as the developed ELISAs were used to screen antibodies [14] or determine the binding domain of the glycoprotein [15]. However, methods have been reported employing Atomic Force Microscopy (AFM) and Surface-Enhanced Raman Spectroscopy (SERS) for detection of FCV with a limits of detection of 3 million and 1million virions/ml, respectively [16].

Biosensors are an attractive detection method for molecules and small particles, such as virions, as they can produce rapid, sensitive and specific signals [17-22]. Both microfluidic and lateral flow assays using liposome nanovesicles as a visual or electrochemical signal generation and amplification system have been well-established using nucleic acids [17-22] and antibodies [23-25] as capture molecules, depending on the target being detected. Additionally, novel biological recognition elements have been employed in similar assays, such as using ganglioside-incorporating liposomes for the detection of cholera toxin subunit B [26].

The often low concentration of virions in water samples, can be a challenge [11]. Addressing this, herein described is the use of a microfluidic device combining pre-concentration and fluorescent detection, previously described [27], to detect FCV. Pre-concentration of the virus particles can be achieved by first allowing liposomes tagged with specific anti-FCV antibodies to bind and then actuating the complexes toward a nanoporous membrane via electrokinetics [27, 28]. These complexes can then be eluted from the membrane as a bolus and applied to a downstream capture and detection zone.

4.3 Materials and methods

4.3.1 Biotinylation of antibodies

Biotin was conjugated to antibodies using the EZ-Link® NHS-PEG₄-Biotin kit and purified using the Slide-A-Lyzer® mini-dialysis kit (Pierce Rockford, IL). Briefly, 100µl of 1mg/ml antibodies were added to the Slide-A-Lyzer tubes and dialyzed against 1XPBS, pH 7.0 to exchange the buffer and assure appropriate pH. Biotin was then added at more than a 20-molar excess to assure good conjugation at the relatively low antibody concentration and the samples were incubated for 30 min at room temperature. The samples were again dialyzed against 1XPBS, pH 7.0 in order to remove the excess biotin. Samples were collected out of the dialysis tubes and stored in the refrigerator.

4.3.2 Preparation of capture beads

Polyclonal anti-FCV antibodies (Baker Institute, Ithaca, NY) were purified from rabbit serum with a HiTrap Protein A HP column (GE Healthcare Uppsala, SE) as per manufacturer suggestions. Once purified, polyclonal antibodies were then conjugated to Protein-A magnetic beads from Dynabeads Immunoprecipitation kit (Invitrogen, Carlsbad, CA) as per manufacturer provided instructions.

4.3.3 Preparation of streptavidin-conjugated liposomes

Fluorescent streptavidin-conjugated liposomes were prepared via the reverse-phase evaporation method using 150mM sulforhodamine B (SRB), 20mM HEPES, pH 7.5

as the encapsulant as previously described [29] with modification. To allow for visualization of the liposomes during the concentration procedure a fluorophore-labeled lipid (Avanti Polar Lipids Alabaster, AL), 0.33mol% 1,2-dipalmitoyl-*sn*-glycero-3-phosphoethanolamine-N-(lissamine rhodamine B sulfonyl), was added to the initial lipid mixture. Liposomes coupled to streptavidin were incubated for 15 minutes at room temperature, with 1µg anti-FCV monoclonal antibody (Abcam Cambridge, MA), biotinylated as above. Liposome-antibody conjugate was then diluted to a working phospholipid concentration of 0.7mM.

Liposomes with the same bilayer composition and streptavidin-modification were also prepared with an encapsulant of potassium ferri/ferrohexacyanide with a combined concentration of 200mM for experiments using amperometric detection. These liposomes were prepared in 1X HEPES-Saline-Sucrose (1XHSS), containing 10mM HEPES, 200mM NaCl, and 200mM sucrose, pH 7.5 but then dialyzed against 1XPBS, 20mM sucrose, pH7.5, as HEPES has been shown to interfere with electrochemistry [30, 31].

4.3.4 Microtiter plate liposome immunoassay (LIA) for antibody selection

Previously reported protocols for the use of liposomes in microtiter [32] were adapted and modified for virus detection. High-binding Nunc Maxisorb® polystyrene plates were prepared for a Liposome Immunoassay (LIA) by washing each well with 200µl of 1X PBS. Anti-FCV antibodies were diluted with 1X PBS to 5µg/ml and 200µl were added to each well. The plates were then incubated overnight in the refrigerator. After incubation, wells were emptied, tapped dry, and washed with 200µl of 1X PBS. Wells were blocked for 1 hour at room temperature with 200µl of blocking reagents

containing either 0.05% Tween-20 or 0.1% Tween-20 in 1X PBS. Plates were then emptied, dried and washed twice with 200µl per well of 1X PBS.

Prepared plates were then loaded with 100µl per well of varying concentrations of FCV in 1X PBS in triplicate and incubated for 2 hours in the refrigerator with gently shaking. Wells were tapped dry and washed twice with 200µl of 1X PBS. Biotinylated anti-FCV antibodies were diluted in 1X PBS to a concentration of 1µg/ml and 100µl were added to each well. Plates were incubated for 1 hour at room temperature, gently shaking.

The plates were washed twice in 200µl per well of 1XHSS. Streptavidin-conjugated liposomes diluted to 50µM phospholipids concentration and 100µl were added to each well. Plates were again incubated for 1 hour at room temperature with gentle shaking.

Plates were emptied, dried, and washed three times with 200µl per well 1X HSS, respectively. For measuring the fluorescence emission at 590nm, 50µl of 30mM octyl-β-D-glucopyranoside (OG) was added to each well.

4.3.5 Concentration and detection of FCV

Prior to performing concentration and detection experiments, the channels of the device, shown in Figure 4.1, were primed with 1XHSS. A permanent magnet was positioned on the top surface of the device upstream of the detection region using adhesive putty. One microliter of polyclonal antibody-conjugated superparamagnetic beads was injected towards the magnet through port 5 using a syringe pump at a flow rate of 1 µl/min. The packed bead bed at the magnet constitutes the capture region of the device. The liposome-antibody conjugate was then mixed with FCV of the required concentration and incubated for two hours. This virus-liposome solution was

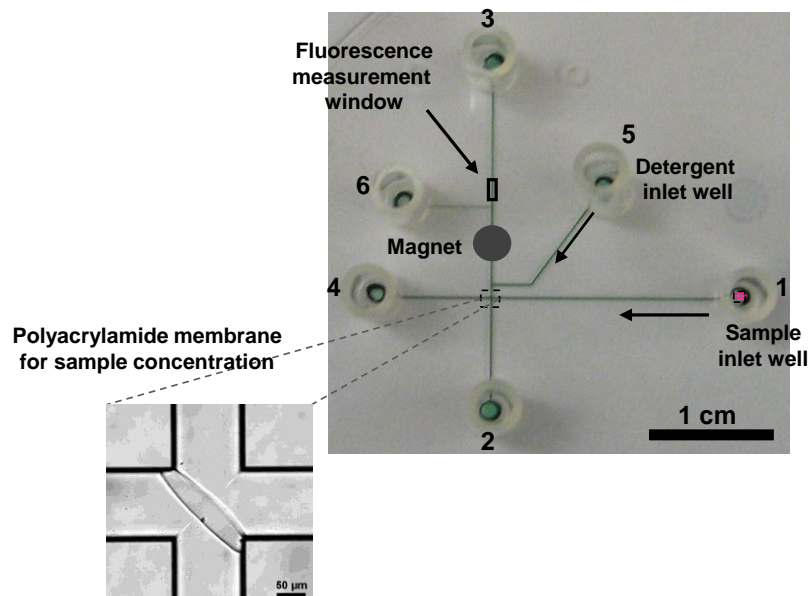


Figure 4.1: Combined Concentration and Detection Device: After the channels are filled with 1XHSS and the capture bead bed is packed at the magnet, a virus-liposome solution is introduced to port 1 and a potential is applied across the membrane (inset). Once concentrated, the virus-liposome bolus is eluted from the membrane by switching the potential to port 3, downstream of the magnet. Once the sample is captured, non-specifically bound liposomes are washed away by wash buffer, applied via port 5 using pressure-driven flow. Liposomes are then lysed using a detergent introduced through the same port.

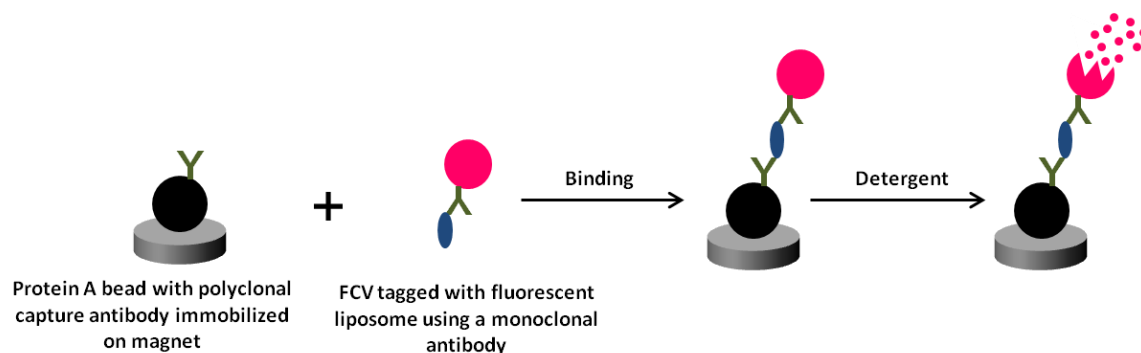


Figure 4.2: Schematic of capture of liposome-virus complex to immobilized magnetic bead in the device and the eventual lysis of the liposome upon flowing detergent.

loaded into the inlet well of the device while all the other wells were filled with 1XHSS. The pressure driven flow in the system was eliminated by adjusting the heights of the solutions in the wells. The virus-liposome complexes were then electrokinetically concentrated at the membrane by applying a voltage difference of 150V across the membrane. After concentrating for a 90 seconds, the concentrated bolus was eluted towards the bead bed by applying a voltage of 150V to the outlet port 3 downstream of the magnet. This results in the capture of the virus-liposome complexes at the bead bed, as illustrated in Figure 4.2. Wash buffer was injected at a flow rate of 20 $\mu\text{l/h}$ to wash off any unbound liposomes in the device through port 5. A detergent solution of 60mM OG was then introduced through the same port towards the bead bed at a flow rate of 40 $\mu\text{l/h}$ and the emitted fluorescence from the lysis of the bound liposomes was recorded downstream of the bead bed. Video was captured during lysis, and the fluorescent intensity was integrated over time to yield the final signal.

4.3.6 Detection of FCV without electrokinetic concentration

To show the effect of pre-concentration on detection of FCV, the assay was also carried out in a polydimethylsiloxane (PDMS) microfluidic channel (Figure 4.3), fabricated via standard soft lithography techniques, and sealed with an interdigitated ultramicroelectrode array (IDUA) fabricated on Pyrex glass, as previously described [33]. The assay without electrokinetic concentration is similar to the procedure outlined above with several modifications required for the electrochemical transducer and pressure-driven flow. Specifically, streptavidin-conjugated liposomes encapsulating the ferri/ferrohexacyanide redox couple were substituted for those encapsulating SRB. Also, 13 μl polyclonal antibody-conjugated superparamagnetic

beads were incubated off-chip with the 70 μ l virus sample for 2 hours, washed 3 times in 1XHSS, and final resuspended in 33 μ l of 1XHSS. These virus-bead complexes were then incubated with 60 μ l of anti-FCV-conjugated liposomes for 1 hour. Of this sample, 10 μ l were loaded into the device at 5 μ l/min until the entire sample was loaded and the beads captured. The flow was continued for 4 minutes in order to wash away any unbound liposomes. As in the case of detection with concentration, 60 μ M OG was injected to lyse the liposomes, here at 1 μ l/min.

Though using a different signal transduction method, previous work has shown detection limits on the same order of magnitude for fluorescent and electrochemical transduction [33].

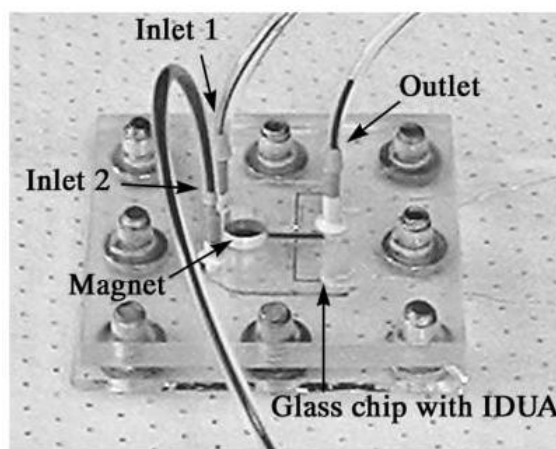


Figure 4.3: Device without pre-concentration module [33]. The device is fabricated by bonding PDMS microchannels to a glass wafer patterned with gold interdigitated electrodes. The entire device was packaged in a Plexiglas[®] housing and provided with inlet and outlet fluidic connections.

4.4 Results and discussion

4.4.1 Selection of antibodies and assay optimization

A series of commercially available and custom antibodies were screened via the microtiter plate LIA described and a sample of highly-purified FCV in PBS. It was found that many antibody pairs would not result in effective capture and detection of FCV. Some pairs generated highly reproducible results and representative data of two combinations are shown in Figure 4.4; here antibody pairs employing the polyclonal antibody as capture antibody generated high signals and signal-to-noise ratios (SNR).

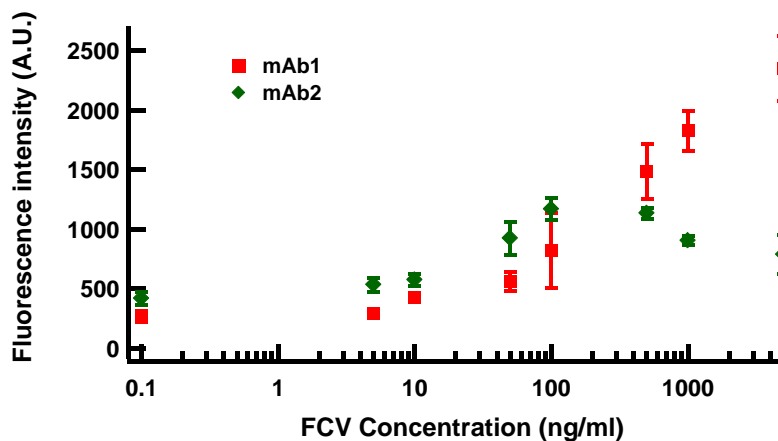


Figure 4.4: Dose-response curves for polyclonal capture antibody with monoclonal reporter antibodies. The best antibody pair for the detection of FCV was determined by screening all variations in a microtiter plate liposome immunoassay (LIA). Here a custom polyclonal anti-FCV was immobilized to the plate and biotinylated anti-FCV monoclonal antibodies and streptavidin-conjugated fluorescent liposomes were used for signal generation.

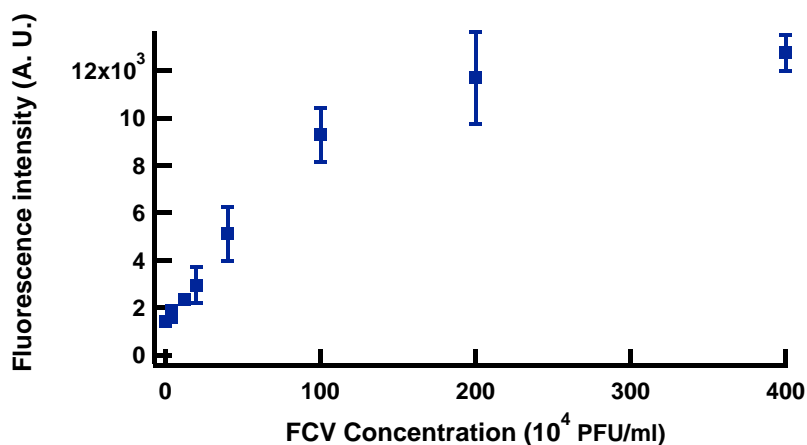


Figure 4.5: Optimized assay for FCV detection in cell culture lysate. Using the previously optimized antibody pairs, FCV was detected in cell culture lysate consisting of DMEM and 10%FBS in a microtiter plate LIA.

Based on all combinations tried, it was determined that using a custom polyclonal rabbit-derived anti-FCV for capture was best in conjunction with the monoclonal labeled “mAb1” (Abcam clone number FCV1-43) as it yielded an SNR just under 9 for a concentration of 5000 ng/ml.

Further optimization of the assay employed FCV in lysed cell culture medium, containing Dulbecco’s Modified Eagle’s Media (DMEM) with 10% fetal bovine serum (FBS), and focused on blocking to reduce non-specific binding. A dose-response curve was developed for the microtiter LIA for future comparison to microfluidic devices, as shown in Figure 4.5. Here, the limit of detection is approximately 4×10^4 PFU/ml (Plaque Forming Units/ml).

4.4.2 Comparison of FCV detection with and without electrokinetic concentration

FCV detection experiments were performed to show the improvement in detection sensitivity with the inclusion of the electrokinetic preconcentration step. In the first set of experiments, FCV was detected using the integrated microfluidic device that includes the preconcentration step. Fluorescent liposomes were used in these experiments and the fluorescence intensity signal from the lysis of the captured liposomes was estimated using image processing. These experiments were done for different concentrations of FCV ranging from 0 – 15 ng/ml (Figure 4.6). The limit of detection for these experiments performed with the integrated device was estimated to be 4 ng/ml or 1.6×10^5 PFU/ml.

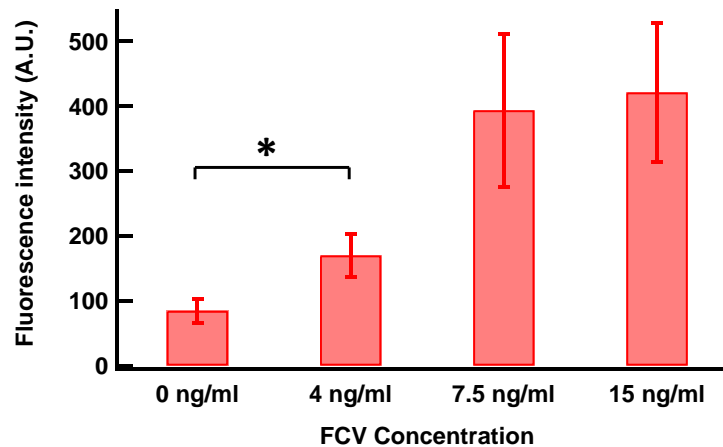


Figure 4.6: FCV detection after electrokinetic concentration. FCV samples were incubated with anti-FCV couple liposomes for two-hours at the indicated concentrations. Samples were then concentrated for 90sec by application of a potential across a nanoporous membrane and then eluted to the capture bead bed. After washing, liposomes were lysed with detergent and the fluorescence intensity downstream was integrated over time. The data is reported as mean \pm SD with $n=3$. * indicates $p<0.05$.

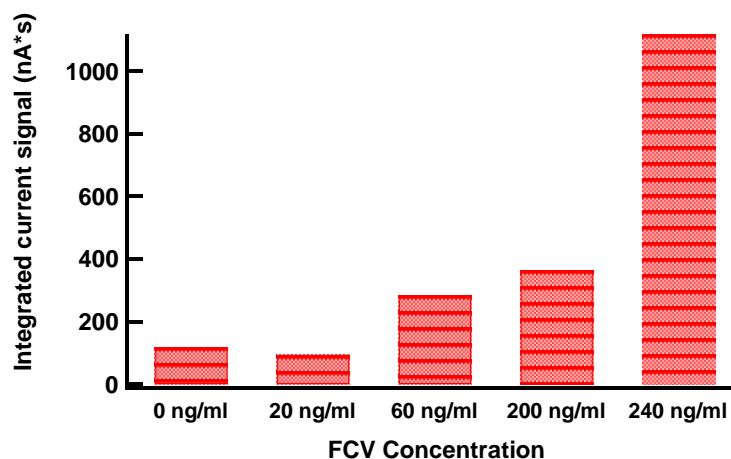


Figure 4.7: FCV detection with direct injection. FCV-magnetic bead complexes were incubated with anti-FCV-conjugated-liposomes off-chip and loaded into the device using a syringe pump. The captured beads were lysed with detergent and the current signal from the released electrochemical markers was quantified.

A second set of experiments were performed excluding the preconcentration step by directly injecting the virus-liposome-bead complexes towards the magnet. Electrochemical liposomes were used in these experiments and the current signal from the lysis of the captured liposomes is plotted as a function of the concentration of FCV as shown in Figure 4.7. The limit of detection in this case was estimated as 60 ng/ml or 2.4×10^6 PFU/ml.

There is an order-of-magnitude improvement in the limit of detection with the integrated microfluidic device over the direct injection system as the increased concentration of the analytes improves the antigen-antibody binding kinetics in the detection region. The preliminary data for direct injection case was generated by incubating the virus sample with the capture beads in suspension of chip, thus allowing a greater surface area for capture. Future experiments will use a pre-packed bead bed for better comparison.

The integrated device can be operated in electrochemical detection mode by patterning gold interdigitated electrodes downstream of the detection region and using

electrochemical liposomes instead of fluorescent liposomes [33]. The equipment needed for electrochemical detection is relatively inexpensive and portable and it can also provide quantitative signal read-out [34].

Current literature reports limits of detection of FCV on the order of 10^6 particles/ml using techniques such as Atomic Force Microscopy (AFM) and Surface Enhanced Raman Spectroscopy (SERS) [16]. Based on an approximate ratio of infectious to non-infectious particles for enteric viruses [35], this corresponds to a limit of detection on the order of 10^4 PFU/ml. Although the limit of detection is lower in this case, the equipment required is bulky and expensive.

Most of the portable microfluidic biosensors for enteric virus detection reported in the literature are based on RT-PCR techniques [36-38]. Apart from the limitation of PCR inhibitors in environmental water samples, microfluidic PCR systems also face the challenges of adsorption of enzymes to channel walls [39], difficulty in precisely controlling temperature, sample evaporation and formation of bubbles in the channels [40]. The advantage of our integrated microfluidic device is that it has on-chip detection times on the order of a few minutes and does not involve any temperature cycling issues.

4.5 Conclusion

In conclusion, we have shown a limit of detection of 1.6×10^5 PFU/ml for Feline Calicivirus using our integrated microfluidic system that combines a membrane-based preconcentration system with liposome-based detection. This detection limit is an order of magnitude lower than that obtained with a device that does not include preconcentration. This device can be extended to operate in electrochemical detection

mode by patterning gold electrodes in the device and using electrochemical liposomes. Electrochemical detection is inexpensive and portable with quantitative signal readout. The on-chip detection time using our microfluidic device is on the order of a few minutes. Also, our device has no temperature cycling issues as opposed to miniaturized PCR-based devices.

Future work involves using electrochemical detection with the integrated microfluidic device by patterning gold electrodes downstream of the detection region in the microfluidic device.

4.6 Acknowledgements

This work was supported by the United States Environmental Protection Agency. The authors would like to thank Dr. John Parker, Associate Professor of Virology Cornell University College of Veterinary Medicine, and his lab at the Baker Institute for Animal Health for supplying virus and polyclonal antibody stock for this work.

BIBLIOGRAPHY

- [1] T.-T. Fong and E. K. Lipp, "Enteric Viruses of Humans and Animals in Aquatic Environments: Health Risks, Detection, and Potential Water Quality Assessment Tools," *Microbiol. Mol. Biol. Rev.*, vol. 69, pp. 357-371, June 1, 2005 2005.
- [2] L. E. Wagenknecht, J. M. Roseman, and W. H. Herman, "Increased incidence of insulin-dependent diabetes mellitus following an epidemic of coxsackievirus B5," *American Journal of Epidemiology*, vol. 133, pp. 1024–1031, 1991.
- [3] F. S. Le Guyader and R. L. Atmar, "Viruses in Shellfish," in *Human Viruses in Water*. vol. 17, A. Bosch, Ed. Amsterdam, The Netherland: Elsevier, 2007, pp. 205-226.
- [4] J. C. Block and L. Schwartzbrod, *Viruses in water systems : detection and identification*. New York, N.Y.; Weinheim, Federal Republic of Germany: VCH Publishers ; VCH Verlagsgesellschaft, 1989.
- [5] R. K. Saiki, D. H. Gelfand, S. Stoffel, S. J. Scharf, R. Higuchi, G. T. Horn, K. B. Mullis, and H. A. Erlich, "Primer-directed enzymatic amplification of DNA with a thermostable DNA polymerase," *Science*, vol. 239, pp. 487-491, January 29, 1988 1988.
- [6] S. U. Parshionikar, S. Willian-True, G. S. Fout, D. E. Robbins, S. A. Seys, J. D. Cassady, and R. Harris, "Waterborne Outbreak of Gastroenteritis Associated with a Norovirus," *Appl. Environ. Microbiol.*, vol. 69, pp. 5263-5268, September 1, 2003 2003.
- [7] D. Pusch, D. Y. Oh, S. Wolf, R. Dumke, U. Schröter-Bobsin, M. Höhne, I. Röske, and E. Schreier, "Detection of enteric viruses and bacterial indicators in German environmental waters," *Archives of Virology*, vol. 150, pp. 929-947, 2005.
- [8] G. S. Fout, B. C. Martinson, M. W. N. Moyer, and D. R. Dahling, "A Multiplex Reverse Transcription-PCR Method for Detection of Human Enteric Viruses in Groundwater," *Appl. Environ. Microbiol.*, vol. 69, pp. 3158-3164, June 1, 2003 2003.
- [9] S. A. Rutjes, H. H. J. L. van den Berg, W. J. Lodder, and A. M. de Roda Husman, "Real-Time Detection of Noroviruses in Surface Water by Use of a Broadly Reactive Nucleic Acid Sequence-Based Amplification Assay," *Appl. Environ. Microbiol.*, vol. 72, pp. 5349-5358, August 1, 2006 2006.

- [10] P. Wyn-Jones, "The Detection of Waterborne Viruses," in *Human Viruses in Water*. vol. 17, A. Bosch, Ed. Amsterdam, The Netherlands: Elsevier, 2007, pp. 177-204.
- [11] J. Jofre, "Indicators of Waterborne Enteric Viruses," in *Human Viruses in Water*. vol. Volume 17, A. Bosch, Ed. Amsterdam, The Netherlands: Elsevier, 2007, pp. 227-249.
- [12] A. Bosch, "Human enteric viruses in the water environment: a minireview," *International Microbiology*, vol. 1, pp. 191-196, 1998.
- [13] J. A. Tree, M. R. Adams, and D. N. Lees, "Disinfection of feline calicivirus (a surrogate for Norovirus) in wastewaters," *Journal of Applied Microbiology*, vol. 98, pp. 155-162, 2005.
- [14] T. Tajima, Y. Takeda, Y. Tohya, and S. Sugii, "Reactivities of Feline Calicivirus Field Isolates with Monoclonal Antibodies Detected by Enzyme-Linked Immunosorbent Assay," *The Journal of Veterinary Medical Science*, vol. 60, pp. 753-755, 1998.
- [15] R. J. Ossiboff and J. S. L. Parker, "Identification of Regions and Residues in Feline Junctional Adhesion Molecule Required for Feline Calicivirus Binding and Infection," *Journal of Virology*, vol. 81, pp. 13608-13621, December 2007 2007.
- [16] M. D. Porter, J. D. Driskell, K. M. Kwarta, R. J. Lipert, J. D. Neill, and J. F. Ridpath, "Detection of Viruses: Atomic Force Microscopy and Surface Enhanced Raman Spectroscopy," *Developments in Biologicals*, vol. 126, pp. 31-39, 2006.
- [17] M. B. Esch, A. J. Baeumner, and R. A. Durst, "Detection of *Cryptosporidium parvum* Using Oligonucleotide-Tagged Liposomes in a Competitive Assay Format," *Analytical Chemistry*, vol. 73, pp. 3162-3167, July 1, 2001 2001.
- [18] H. A. Hartley and A. J. Baeumner, "Biosensor for the Specific Detection of a Single Viable *B. anthracis* Spore," *Analytical and Bioanalytical Chemistry*, vol. 376, pp. 319-327, 2003.
- [19] J. Connelly, S. Nugen, W. Borejsza-Wysocki, R. Durst, R. Montagna, and A. Baeumner, "Human pathogenic *Cryptosporidium* species bioanalytical detection method with single oocyst detection capability," *Analytical and Bioanalytical Chemistry*, vol. 391, pp. 487-495, 2008.
- [20] A. J. Baeumner, N. A. Schlesinger, N. S. Slutzki, J. Romano, E. M. Lee, and R. A. Montagna, "A Biosensor for Dengue Virus Detection: Sensitive, Rapid and Serotype specific," *Analytical Chemistry*, vol. 74, pp. 1442 – 1448, March 22, 2002 2002.

- [21] N. V. Zaytseva, R. A. Montagna, E. M. Lee, and A. J. Baeumner, "Multi-analyte single-membrane biosensor for the serotype-specific detection of Dengue virus," *Analytical and Bioanalytical Chemistry*, pp. 46-53, 2004.
- [22] A. J. Baeumner, R. N. Cohen, V. Miksic, and J. H. Min, "RNA Biosensor for the Rapid Detection of Viable *Escherichia coli* in Drinking Water," *Biosensors & Bioelectronics*, vol. 8, pp. 405 – 419, 2003.
- [23] T. DeCory, R. A. Durst, S. Zimmerman, L. Garringer, G. Paluca, H. DeCory, and R. A. Montagna, "Development of an Immunomagnetic Bead-Immunoliposome Fluorescence Assay for Rapid Detection of *Escherichia coli* O157:H7 in Aqueous Samples and Comparison of the Assay with Standard Microbiology Method," *Applied and Environmental Microbiology*, vol. 71, pp. 1856-1864, April 2005 2005.
- [24] M. Kim, S. Oh, and R. A. Durst, "Detection of *Escherichia coli* O157:H7 Using Combined Procedure of Immunomagnetic Separation and Test Strip Liposome Immunoassay," *Journal of Microbiology and Biotechnology*, vol. 13, pp. 509-516, 2003.
- [25] S. Park and R. A. Durst, "Modified Immunoliposome Sandwich Assay for the Detection of *Escherichia coli* O157:H7 in Apple Cider," *Journal of Food Protection*, vol. 67, pp. 1568-1573, 2004.
- [26] N. Bunyakul, K. Edwards, C. Promptmas, and A. Baeumner, "Cholera toxin subunit B detection in microfluidic devices," *Analytical and Bioanalytical Chemistry*, 2008.
- [27] S. Kondapalli, J. T. Connelly, A. J. Baeumner, and B. J. Kirby, "Integrated microfluidic preconcentrator and immunobiosensor for pathogen detection," *in preparation*, 2011.
- [28] S. Song, A. K. Singh, and B. J. Kirby, "Electrophoretic Concentration of Proteins at Laser-Patterned Nanoporous Membranes in Microchips," *Anal. Chem.*, vol. 76, pp. 4589-4592, 2004.
- [29] K. Edwards, K. Curtis, J. Sailor, and A. Baeumner, "Universal liposomes: preparation and usage for the detection of mRNA," *Analytical and Bioanalytical Chemistry*, vol. 391, pp. 1689-1702, 2008.
- [30] J.-F. Masson, E. Gauda, B. Mizaikoff, and C. Kranz, "The interference of HEPES buffer during amperometric detection of ATP in clinical applications," *Analytical & Bioanalytical Chemistry*, vol. 390, pp. 2067-2071, 2008.
- [31] K. D. Welch, T. Z. Davis, and S. D. Aust, "Iron Autoxidation and Free Radical Generation: Effects of Buffers, Ligands, and Chelators," *Archives of Biochemistry and Biophysics*, vol. 397, pp. 360-369, 2002.

- [32] K. A. Edwards and A. J. Baeumner, "Optimization of DNA-tagged liposomes for use in microtiter plate analyses," *Analytical & Bioanalytical Chemistry*, vol. 386, pp. 1613-1623, 2006.
- [33] V. N. Goral, N. V. Zaytseva, and A. J. Baeumner, "Electrochemical microfluidic biosensor for the detection of nucleic acid sequences," *Lab on a Chip*, vol. 6, pp. 414-421, 2006.
- [34] S. Kwakye and A. Baeumner, "An embedded system for portable electrochemical detection," *Sens. Actuators, B*, vol. B123, pp. 336-343, 2007.
- [35] H. Kopecka, S. Dubrou, J. Prevot, J. Marechal, and J. M. Lopez-Pila, "Detection of naturally occurring enteroviruses in waters by reverse transcription, polymerase chain reaction, and hybridization," *Appl. Environ. Microbiol.*, vol. 59, pp. 1213-19, 1993.
- [36] W.-C. Lee, K.-Y. Lien, G.-B. Lee, and H.-Y. Lei, "An integrated microfluidic system using magnetic beads for virus detection," *Diagn. Microbiol. Infect. Dis.*, vol. 60, pp. 51-58, 2008.
- [37] Y. Li, C. Zhang, and D. Xing, "Fast identification of foodborne pathogenic viruses using continuous-flow reverse transcription-PCR with fluorescence detection," *Microfluid. Nanofluid.*, vol. 10, pp. 367-380, 2011.
- [38] K.-Y. Lien, W.-C. Lee, H.-Y. Lei, and G.-B. Lee, "Integrated reverse transcription polymerase chain reaction systems for virus detection," *Biosens. Bioelectron.*, vol. 22, pp. 1739-1748, 2007.
- [39] C. Zhang, J. Xu, W. Ma, and W. Zheng, "PCR microfluidic devices for DNA amplification," *Biotechnol. Adv.*, vol. 24, pp. 243-284, 2006.
- [40] C. Zhang and D. Xing, "Miniaturized PCR chips for nucleic acid amplification and analysis: latest advances and future trends," *Nucleic Acids Res.*, vol. 35, pp. 4223-4237, 2007.

CHAPTER 5

CONCLUSION

In this work, we have shown the use of microfluidic control in two different biological applications. In the first application, we developed a microfluidic device that has the potential to automate combinatorial processes like protein refolding. This device uses pneumatic valves and pumps that can be actuated in an automated fashion to enable the process of choosing specific amounts of reagents for mixing. We have also shown on-chip assay compatibility for quantifying refolding yields. In the second application, we developed an integrated microfluidic device for enteric virus detection in water samples. This device integrates membrane-based preconcentration with liposome-based signal amplification. We used this device for the detection of Feline Calicivirus, which is a model system for human enteric virus, in water samples.

5.1 Summary of accomplishments

The intended goal for the protein refolding work was to develop a microfluidic device that can automate the combinatorial process of finding the right solution conditions to properly refold proteins to their native functional state. In **Chapter 2**, we have described in detail our fabrication process for making this two-layered PDMS-on-glass device with flow and control channels [1]. The flow of the reagents in the flow channels was controlled by pneumatically actuating the control channels. Each flow channel was equipped with a valve and a pump to control the choice and amount of the reagents injected into the rotary mixer [2]. The pneumatic actuation of the valves

and pumps was automated by connecting them to a valve manifold which was controlled using a Lab view program. The flow rate of the reagent in the flow channel is a function of the actuation frequency of the pump. As the frequency of actuation increases, the flow rate also increases initially but at higher frequencies, the flow rate decreases due to incomplete valve opening/closing. A frequency of 10 Hz was estimated as the optimal frequency for the highest flow rate. By controlling this frequency and the time for which the pump is operated, the amount of the reagent injected into the rotary mixer can be precisely controlled. We also performed dye-mixing experiments in the device by injecting two food dyes into the rotary mixer and actuating the pump on the mixer. The total time taken for mixing was estimated as 45s. Refolding experiments were performed on the protein β -galactosidase and the refolding yield was quantified using a fluorometric assay fluorescein di- β -D-galactopyranoside (FDG) as the substrate [3, 4]. For on-chip quantification of refolding yield, different concentrations of β -galactosidase were mixed with FDG and the fluorescence intensity of the protein-FDG mixture in a PDMS microchannel was estimated using image processing tools to obtain a calibration curve. Multiple denaturing and refolding experiments were performed on the protein using optimized protocols [5] and using the calibration curve, the active protein content was estimated in the denatured and refolded samples. The refolding yields obtained in these trials were on the order of 37%, comparable to yields reported in the literature for β -galactosidase [5]. Since the device is optically clear, it is also compatible with various techniques to study refolding intermediates like small-angle x-ray scattering [6] and terahertz spectroscopy [7].

The intended goal of the virus detection project was to develop a portable inexpensive microfluidic biosensor that can serve as an early screening system for the detection of enteric viruses in environmental water samples. This is to overcome the

limitations of conventional methods of enteric virus detection like long culture times for cell-culture methods and extensive sample preparation requirements for PCR-based methods [8-10]. In **Chapter 3**, we describe the design of our integrated microfluidic biosensor that combines on-chip preconcentration with liposome-based signal amplification. The device was made by etching microchannels in a glass wafer and bonding it to another glass wafer using a low-temperature bonding technique [11-14]. A nanoporous membrane was fabricated at the junction of the microchannels by an *in situ* laser polymerization technique [15-19]. By applying an electric field across the membrane, analytes of interest were electrophoretically migrated towards the membrane and concentrated by sieving effect. The performance of the membrane was characterized by estimating the concentration factors during liposome concentration as a function of the time for which an electric field is applied across the membrane. After 160s of applying an electric field across the membrane, two orders of magnitude concentration was obtained in this system. The concentrated bolus of liposomes was eluted by switching the electric field towards a detection region downstream. The captured liposomes were then lysed by flowing a detergent and released fluorescence was quantified.

In order to estimate the effect of the preconcentration system on device performance, two sets of experiments were performed using biotin-streptavidin binding as a model system. In the first set of experiments, biotinylated liposomes were electrophoretically concentrated for 90s and eluted towards a bed of streptavidin-conjugated magnetic beads immobilized at a magnet. In the second set of experiments, the biotinylated liposomes were directly injected towards the bead bed without any preconcentration. The same number of liposomes was used in both experiments for comparison. From these experiments, it was concluded that the inclusion of the

preconcentration system results in a fourteen-fold improvement in the signal as opposed to a device without preconcentration.

In **Chapter 4**, we used the integrated device for detection of Feline Calicivirus (FCV), which is a model system for human enteric virus [20]. FCV was captured in a sandwich immunoassay in the device using two sets of antibodies. Protein A beads coated with a polyclonal capture antibody and immobilized at the magnet serve as the capture region. FCV was tagged to fluorescent liposomes using monoclonal probe antibodies off-chip. The antibody pair for the best signals was determined by performing microtiter plate assays with different antibody pair combinations. Monoclonal probe antibody from Abcam and polyclonal capture antibody was determined as the best pair for highest signal-to-noise ratios. On-chip detection experiments with the integrated device resulted in a limit of detection (LOD) on the order of 1.6×10^5 PFU/ml which was an order of magnitude lower than the LOD obtained using a device without preconcentration. The device can be extended to operate in electrochemical detection mode, making it an inexpensive and portable alternative to existing techniques like AFM and SERS [21]. This technique also does not include any temperature cycling issues as opposed to existing microfluidic PCR devices [22, 23].

5.2 Future work

Future work for the protein refolding project involves performing on-chip refolding assays of β -galactosidase by combinatorially choosing reagents in the three-input design. In the off-chip refolding protocol for β -galactosidase, in order to obtain the maximum refolding yields, 1mM MgCl_2 and 1.4M urea were used in the refolding

buffer and the protein was diluted in 1:12 dilution ratio in this buffer [5]. For the initial on-chip experiments, the concentrations of these two reagents (MgCl_2 and urea) can be varied along with the dilution ratio to estimate the optimal conditions for refolding. Also, since the refolding protocol involves long incubation times, the device will have to be placed in a water bath to prevent evaporation of the reagents from the PDMS channels.

For the next set of experiments, the number of input channels on the rotary mixer in the PDMS –glass device can be increased to include more reagents like sodium phosphate and DTE (dithioerythritol). The effect of the individual reagents on the refolding yield as well as the effect of a combination of reagents can be evaluated. In the current design, each input flow channel is independently controlled by a valve and pump to control the choice and amount of reagent being injected into the rotary mixer. However, with this configuration, as the system is scaled-up to include more input channels, the number of valves and pumps required to control the flow channels also scales up linearly. In other words, for n flow channels, the number of control channels scales up as $3n$ (for pumps) + n (for valves). On the other hand, Thorsen *et al.*[24] used combinatorial arrays of binary valve patterns for large-scale integration of microfluidic channel networks. For this system, the number of control channels required to control n flow channels scales as $2\log_2 n$. Thus, only 20 control channels are required to control 1024 flow channels. The device design will be changed to such a valve pattern to realize large-scale integration with multiple inlet flow channels.

For the virus detection project, the next step is to extend the device for use in electrochemical detection format by patterning gold electrodes downstream from the capture region in the device [25]. For these experiments, electrochemical liposomes with potassium ferri/ferrohexacyanide molecules will be used for signal amplification instead of fluorescent liposomes. These electrochemical markers undergo a cyclic

redox reaction at the gold interdigitated electrodes and generate a current signal that can be measured using a minipotentiostat. The use of such a minipotentiostat to make electrochemical measurements will be explored to show the portability of the biosensor [26]. The limiting step in using the device in the electrochemical detection mode is the fabrication and integration of the gold interdigitated electrodes in the glass device. We chose a low-temperature sol-gel based method for bonding glass wafers [12-14] as the conventional high-temperature methods lead to delamination of the patterned gold electrodes. However, the extensive pre-cleaning steps for glass wafers before bonding have been causing gold delamination issues. This can be overcome by improving the adhesion of the patterned gold to glass wafers and also using milder pre-cleaning steps before bonding. Different adhesion layers (like Chromium or Titanium) and diffusion barriers (like Platinum) can be used to improve the adhesion of gold to glass wafers.

The current limit of detection of our integrated biosensor for Feline Calicivirus is 1.6×10^5 PFU/ml. However, environmental water samples contain enteric viruses at a much lower concentration (100 PFU/l on an average [8], which translates to about 75 PFU/ml after using electropositive cartridge filters for concentration, which have about 75% recovery efficiency [27-29]). In order to further improve the limit of detection of our device, multiple concentration-elution sequences can be performed to capture more analytes. Also, the channel layout in the device can be redesigned to further decrease the distance between the concentration and detection modules to reduce the effects of dispersion.

In the current protocol for FCV detection using the integrated immunobiosensor, FCV is tagged with the liposome-antibody conjugate by incubating off-chip for two hours. Although the on-chip detection times using the biosensor are much lower compared to other techniques like RT-PCR [30-32], the total analysis time

is still high due to the off-chip incubation step. The time for this incubation step can be reduced by introducing a mixing region on-chip for tagging FCV with liposome-antibody conjugate. On-chip mixing can be achieved by using serpentine channels in the device.

Finally, the device will be tested for use with environmental water samples by performing control experiments with water spiked with model contaminants.

Examples of model contaminants that can be used include humic acid, sea salts and fine test dust. These contaminants help to identify specific parts of the device that may fail upon repeated use. The humic acid has a tendency to adhere to channel walls and this tests the effectiveness of the polyacrylamide coating used to prevent adhesion on the channel walls. Sea salts increase the conductivity of the buffer and thereby affect the electric fields applied in the system during concentration-elution. They may also interfere with the current signals during electrochemical detection. The test dust may clog the pores of the nanoporous membrane and reduce the concentration efficiency. By performing controlled tests with these model contaminants, we can determine the level of sample preprocessing needed before it is introduced into the device and also get an estimate of the number of times the device can be repeatedly used before it fails.

BIBLIOGRAPHY

- [1] M. A. Unger, H.-P. Chou, T. Thorsen, A. Scherer, and S. R. Quake, "Monolithic microfabricated valves and pumps by multilayer soft lithography," *Science (Washington, D. C.)*, vol. 288, pp. 113-116, 2000.
- [2] H.-P. Chou, M. A. Unger, and S. R. Quake, "A microfabricated rotary pump," *Biomedical Microdevices*, vol. 3, pp. 323-330, 2001.
- [3] G. P. Nolan, S. Fiering, J. F. Nicolas, and L. A. Herzenberg, "Fluorescence-activated cell analysis and sorting of viable mammalian cells based on b-D-galactosidase activity after transduction of *Escherichia coli* lacZ," *Proceedings of the National Academy of Sciences of the United States of America*, vol. 85, pp. 2603-7, 1988.
- [4] B. Rotman, J. A. Zderic, and M. Edelstein, "Fluorogenic substrates for b-D-galactosidases and phosphatases derived from fluorescein (3,6-dihydroxyfluoran) and its mono-methyl ether," *Proceedings of the National Academy of Sciences of the United States of America*, vol. 50, pp. 1-6, 1963.
- [5] A. Nichtl, J. Buchner, R. Jaenicke, R. Rudolph, and T. Scheibel, "Folding and association of b-galactosidase," *Journal of Molecular Biology*, vol. 282, pp. 1083-1091, 1998.
- [6] L. Pollack, M. W. Tate, A. C. Finnefrock, C. Kalidas, S. Trotter, N. C. Darnton, L. Lurio, R. H. Austin, C. A. Batt, S. M. Gruner, and S. G. J. Mochrie, "Time resolved collapse of a folding protein observed with small angle X-ray scattering," *Physical Review Letters*, vol. 86, pp. 4962-4965, 2001.
- [7] P. A. George, W. Hui, F. Rana, B. G. Hawkins, A. E. Smith, and B. J. Kirby, "Microfluidic devices for terahertz spectroscopy of biomolecules," *Optics Express*, vol. 16, pp. 1577-1582, 2008.
- [8] T. G. Metcalf, J. L. Melnick, and M. K. Estes, "Environmental virology: from detection of virus in sewage and water by isolation to identification by molecular biology - a trip of over 50 years," *Annu. Rev. Microbiol.*, vol. 49, pp. 461-87, 1995.
- [9] M. M. Ijzerman, D. R. Dahling, and G. S. Fout, "A method to remove environmental inhibitors prior to the detection of waterborne enteric viruses by reverse transcription-polymerase chain reaction," *J. Virol. Methods*, vol. 63, pp. 145-153, 1997.

- [10] Y. S. C. Shieh, D. Wait, L. Tai, and M. D. Sobsey, "Methods to remove inhibitors in sewage and other fecal wastes for enterovirus detection by the polymerase chain reaction," *J. Virol. Methods*, vol. 54, pp. 51-66, 1995.
- [11] H. Y. Wang, R. S. Foote, S. C. Jacobson, J. H. Schneibel, and J. M. Ramsey, "Low temperature bonding for microfabrication of chemical analysis devices," *Sens. Actuators, B*, vol. B45, pp. 199-207, 1997.
- [12] J. Khandurina, S. C. Jacobson, L. C. Waters, R. S. Foote, and J. M. Ramsey, "Microfabricated Porous Membrane Structure for Sample Concentration and Electrophoretic Analysis," *Anal. Chem.*, vol. 71, pp. 1815-1819, 1999.
- [13] J. Khandurina, T. E. McKnight, S. C. Jacobson, L. C. Waters, R. S. Foote, and J. M. Ramsey, "Integrated system for rapid PCR-based DNA analysis in microfluidic devices," *Anal. Chem.*, vol. 72, pp. 2995-3000, 2000.
- [14] R. S. Foote, J. Khandurina, S. C. Jacobson, and J. M. Ramsey, "Preconcentration of proteins on microfluidic devices using porous silica membranes," *Anal. Chem.*, vol. 77, pp. 57-63, 2005.
- [15] D. J. Throckmorton, T. J. Shepodd, and A. K. Singh, "Electrochromatography in microchips: reversed-phase separation of peptides and amino acids using photopatterned rigid polymer monoliths," *Anal. Chem.*, vol. 74, pp. 784-789, 2002.
- [16] A. E. Herr and A. K. Singh, "Photopolymerized Cross-Linked Polyacrylamide Gels for On-Chip Protein Sizing," *Anal. Chem.*, vol. 76, pp. 4727-4733, 2004.
- [17] S. Song, A. K. Singh, and B. J. Kirby, "Electrophoretic Concentration of Proteins at Laser-Patterned Nanoporous Membranes in Microchips," *Anal. Chem.*, vol. 76, pp. 4589-4592, 2004.
- [18] S. Song, A. K. Singh, T. J. Shepodd, and B. J. Kirby, "Microchip dialysis of proteins using in situ photopatterned nanoporous polymer membranes," *Anal. Chem.*, vol. 76, pp. 2367-2373, 2004.
- [19] A. V. Hatch, A. E. Herr, D. J. Throckmorton, J. S. Brennan, and A. K. Singh, "Integrated Preconcentration SDS-PAGE of Proteins in Microchips Using Photopatterned Cross-Linked Polyacrylamide Gels," *Anal. Chem.*, vol. 78, pp. 4976-4984, 2006.
- [20] J. A. Tree, M. R. Adams, and D. N. Lees, "Disinfection of feline calicivirus (a surrogate for Norovirus) in wastewaters," *J. Appl. Microbiol.*, vol. 98, pp. 155-162, 2005.
- [21] M. D. Porter, J. D. Driskell, K. M. Kwarta, R. J. Lipert, J. D. Neill, and J. F. Ridpath, "Detection of Viruses: Atomic Force Microscopy and Surface

- Enhanced Raman Spectroscopy," *Developments in Biologicals*, vol. 126, pp. 31-39, 2006.
- [22] C. Zhang and D. Xing, "Miniaturized PCR chips for nucleic acid amplification and analysis: latest advances and future trends," *Nucleic Acids Res.*, vol. 35, pp. 4223-4237, 2007.
 - [23] C. Zhang, J. Xu, W. Ma, and W. Zheng, "PCR microfluidic devices for DNA amplification," *Biotechnol. Adv.*, vol. 24, pp. 243-284, 2006.
 - [24] T. Thorsen, S. J. Maerkl, and S. R. Quake, "Microfluidic Large-Scale Integration," *Science (Washington, DC, United States)*, vol. 298, pp. 580-584, 2002.
 - [25] V. N. Goral, N. V. Zaytseva, and A. J. Baeumner, "Electrochemical microfluidic biosensor for the detection of nucleic acid sequences," *Lab on a Chip*, vol. 6, pp. 414-421, 2006.
 - [26] S. Kwakye and A. Baeumner, "An embedded system for portable electrochemical detection," *Sens. Actuators, B*, vol. B123, pp. 336-343, 2007.
 - [27] M. D. Sobsey and J. S. Glass, "Poliovirus concentration from tap water with electropositive adsorbent filters," *Appl Environ Microbiol*, vol. 40, pp. 201-10, 1980.
 - [28] M. R. Karim, E. R. Rhodes, N. Brinkman, L. Wymer, and G. S. Fout, "New electropositive filter for concentrating enteroviruses and noroviruses from large volumes of water," *Appl. Environ. Microbiol.*, vol. 75, pp. 2393-2399, 2009.
 - [29] C. D. Gibbons, R. A. Rodriguez, L. Tallon, and M. D. Sobsey, "Evaluation of positively charged alumina nanofibre cartridge filters for the primary concentration of noroviruses, adenoviruses and male-specific coliphages from seawater," *J. Appl. Microbiol.*, vol. 109, pp. 635-641, 2010.
 - [30] W.-C. Lee, K.-Y. Lien, G.-B. Lee, and H.-Y. Lei, "An integrated microfluidic system using magnetic beads for virus detection," *Diagn. Microbiol. Infect. Dis.*, vol. 60, pp. 51-58, 2008.
 - [31] Y. Li, C. Zhang, and D. Xing, "Fast identification of foodborne pathogenic viruses using continuous-flow reverse transcription-PCR with fluorescence detection," *Microfluid. Nanofluid.*, vol. 10, pp. 367-380, 2011.
 - [32] K.-Y. Lien, W.-C. Lee, H.-Y. Lei, and G.-B. Lee, "Integrated reverse transcription polymerase chain reaction systems for virus detection," *Biosens. Bioelectron.*, vol. 22, pp. 1739-1748, 2007.